Chinese Medicine

RESEARCH

Open Access

Quality assessment and Q-markers discovery of Tongsaimai tablet by integrating serum pharmacochemistry and network pharmacology for anti-atherosclerosis benefit

Yanfen Cheng[1†], Meng Xiao[1†], Jiamei Chen[1], Di Wang[1], Yichen Hu[2], Chenfeng Zhang[3,4], Tuanjie Wang[3,4], Chaomei Fu[1], Yihan Wu[1*] and Jinming Zhang[1*]

Abstract

Background: The limited therapeutic outcomes of atherosclerosis (AS) have allowed, traditional Chinese medicine has been well established as an alternative approach in ameliorating AS and associated clinical syndromes. Clinically, Tongsaimai tablet (TSMT), a commercial Chinese patent medicine approved by CFDA, shows an obvious therapeutic effect on AS treatment. However, its effective mechanism and quality control still need thorough and urgent exploration.

Methods: The mice were orally administered with TSMT and their serum was investigated for the absorbed compounds using serum pharmacochemistry via the UPLC-Q-Exactive Orbitrap/MS analysis was employed to investigate these absorbed compounds in serum of mice orally administrated with TSMT. Based on these absorbed prototype compounds in serum derived from TSMT, a component-target-disease network was constructed using network pharmacology strategy, which elucidated the potential bioactive components, effective targets, and molecular mechanisms of TSMT against AS. Further, the screened compounds from the component-target network were utilized as the quality control (QC) markers, determining multi-component content determination and HPLC fingerprint to assess quality of nine batches of TSMT samples.

Results: A total of 164 individual components were identified in TSMT. Among them, 29 prototype compounds were found in serum of mice administrated with TSMT. Based on these candidate prototype components, 34 protein targets and 151 pathways related to AS were predicted, and they might significantly exhibit potential anti-AS mechanisms via synergistic regulations of lipid regulation, shear stress, and anti-inflammation, etc. Five potentially bioactive ingredients in TSMT, including Ferulic acid, Liquiritin, Senkyunolide I, Luteolin and Glycyrrhizic acid in quantity not less than 1.2798, 0.4716, 0.5419, 0.1349, 4.0386 mg/g, respectively, screened from the component-target-pathway network. Thereby, these indicated that these five compounds of TMST which played vital roles in the attenuation of AS could serve as crucial marker compounds for quality control.

[†]Yanfen Cheng and Meng Xiao contributed equally to this work

*Correspondence: yihanwuone@126.com; zhangjinming1987@126.com

[1] State Key Laboratory of Southwestern Chinese Medicine Resources, School of Pharmacy, Chengdu University of Traditional Chinese Medicine, Chengdu 611137, China
Full list of author information is available at the end of the article

Conclusions: Overall, based on the combination of serum pharmacochemistry and network pharmacology, the present study firstly provided a useful strategy to establish a quality assessment approach for TSMT by screening out the potential anti-AS mechanisms and chemical quality markers.

Keywords: Tongsaimai tablet, Quality control, Serum pharmacochemistry, Network pharmacology, Atherosclerosis, Q-markers

Graphical Abstract

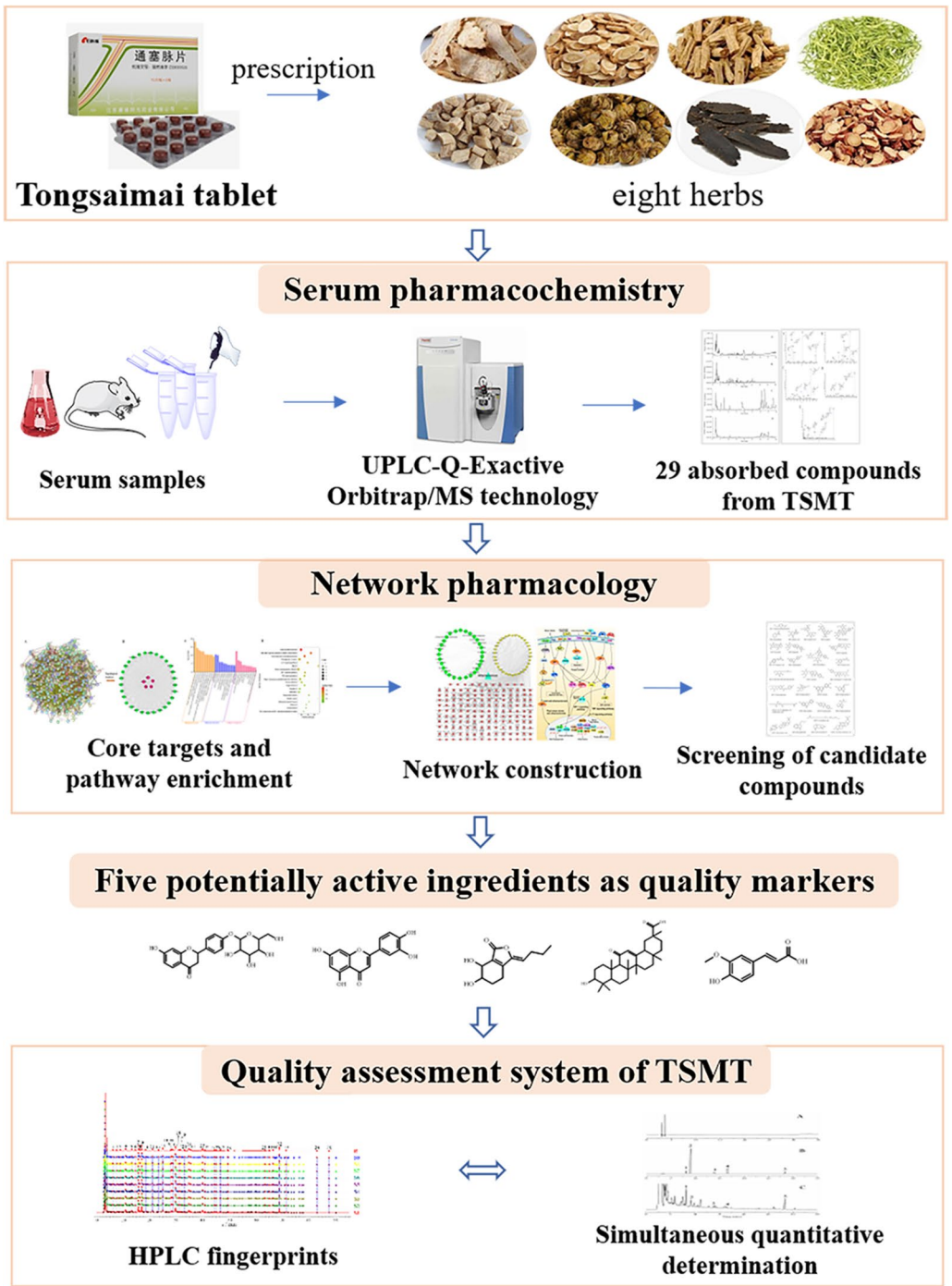

Introduction

Atherosclerosis (AS) is presented as the main pathological process in the heart, brain, and peripheral vascular diseases. It is characterized by the accumulation of pathological plaque and inflammation of the arterial wall [1]. AS also remains the leading cause of morbidity and mortality worldwide and may induce coronary heart disease, thrombosis, stroke, cerebrovascular infarction and other related serious complications [2]. Due to the insufficient therapeutic outcomes and potential side effects of commercial medicines such as statins [3], traditional Chinese medicine (TCM) are being increasingly recommended for the prevention and treatment of AS. Some Chinese patent medicines, such as Xue Zhi Kang Capsule and Shan Zha Jian Zhi tablet along with their bioactive herbal components, namely Ginkgolides and tanshinones, have exhibited significant efficacy in clinical or pre-clinical studies [4, 5].

Based on TCM theory, Tongsaimai tablet (TSMT), a commercial Chinese patent medicine, exhibits the medicinal function of promoting blood circulation, dredging collaterals, tonifying Qi, and nourishing Yin [6]. TSMT has been commonly applied to improve these clinical symptoms associated with AS, including regulation of inflammation, stabilization of plaque, protection of vascular endothelial cells, regulation of blood lipid, inhibition of blood coagulation, and so on [7–9]. Furthermore, the herbs in the prescription of TSMT, namely *Angelica sinensis* (Oliv.) Diels, *Lonicera japonica* Thunb., *Codonopsis pilosula* (Franch.) Nannf., *Scrophularia aestivalis* Griseb, *Astragalus membranaceus* (Fisch.) Bunge, *Achyranthes bidentata* Bl., *Dendrobium nobile* Lindl., and *Glycyrrhiza uralensis* Fisch., ameliorated AS or peripheral vascular diseases. However, only a few studies have investigated the mechanisms of TSMT in ameliorating AS. Moreover, despite the affirmed clinical benefits of TSMT, its quality control and assessment remain greatly limited. Based on the mandatory quality control standards, the only the recommended quantitative determination was of chlorogenic acid, which was mainly derived from *Lonicera japonica* Thunb. [10]. The holistic view of TCM theory believes that traditional Chinese medicinal herbs work via the complex interactions among the complex disease targets and a variety of chemical constituents [11]. However, exploring the ingredients responsible for therapeutic efficacy remains a matter of concern. Unfortunately, the current quality control index of chlorogenic acid cannot represent the effective material basis for TSMT. Therefore, there is a need to promote rational quality assessment of TSMT based on the real quality control markers.

Since it is a well-acknowledged viewpoint that only the components absorbed into serum are the potential bioactive material basis of medicinal herbs [12], we used serum pharmacochemistry to analyze the prototype phytochemical compounds in TSMT prescription. As a proof of concept, the absorbed phytochemical constituents of TSMT in mice serum were identified using a UPLC-Q-Exactive Orbitrap/MS analysis approach. Next, serum pharmacochemistry integrated with network pharmacology [11] was used to examine the potentially active components in TSMT and their possible mechanisms ameliorating AS. This approach has also been corroborated as a useful approach in our previous study [13]. Based on the predicted effective phytochemicals in TSMT, we developed both the quantitative determination of multiple components by HPLC and chromatographic fingerprint to assess the quality of multiple batches of TSMT samples. To the best of our knowledge, this is the first report to explore the quality control aspect of TSMT based on the potential effective compounds and their therapeutic benefits. Figure 1 depicts the schematic representation of the study.

Materials and methods

Materials and chemicals

We obtained the nine batches of TSMT samples (S1-S9, No. 210401 ~ 210409) from Jiangsu Kanion Pharmaceutical Co., Ltd (Jiangsu, China). These were prepared from eight herbal pieces, i.e., *Angelica sinensis* (Oliv.) Diels (DG, danggui), *Lonicera japonica* Thunb. (JYH, jinyinhua), *Codonopsis pilosula* (Franch.) Nannf. (DS, dangshen), *Scrophularia aestivalis* Griseb (XS, xuanshen), *Astragalus membranaceus* (Fisch.) Bunge (HQ, huangqi), *Achyranthes bidentata* Bl. (NX, niuxi), *Dendrobium nobile* Lindl. (SH, shihu), and *Glycyrrhiza uralensis* Fisch. (GC, gancao) which were also checked with http://www.theplantlist.org on February 14, 2022. Next, we purchased 17 reference standards (RS) from Chengdu MUST Bio-Technology Co, Ltd (Chengdu, China), which included Astragaloside IV, Calycosin-7-glucoside, Atractylenolide II, Atractylenolide III, Ferulic acid, Senkyunolide I, Cynaroside, Chlorogenic acid, Luteolin, Harpagoside, Harpgide, Acteoside, β-Ecdysone, Ginsenoside Ro, Glycyrrhizic acid, Liquiritin, and Gallic acid. The purity of all the reference standards was over 98%. Mobile phases including the HPLC-grade acetonitrile, phosphoric acid, and formic acid were purchased from Thermo Fisher Scientific (Thermo scientific, USA).

Preparation of standards and TSMT samples

For qualitative identification of the chemicals, all reference standards were dissolved in methanol for the UPLC-Q-Exactive Orbitrap/MS analysis. Additionally, for HPLC fingerprint and content determination analysis, the mixed reference solution was prepared including five

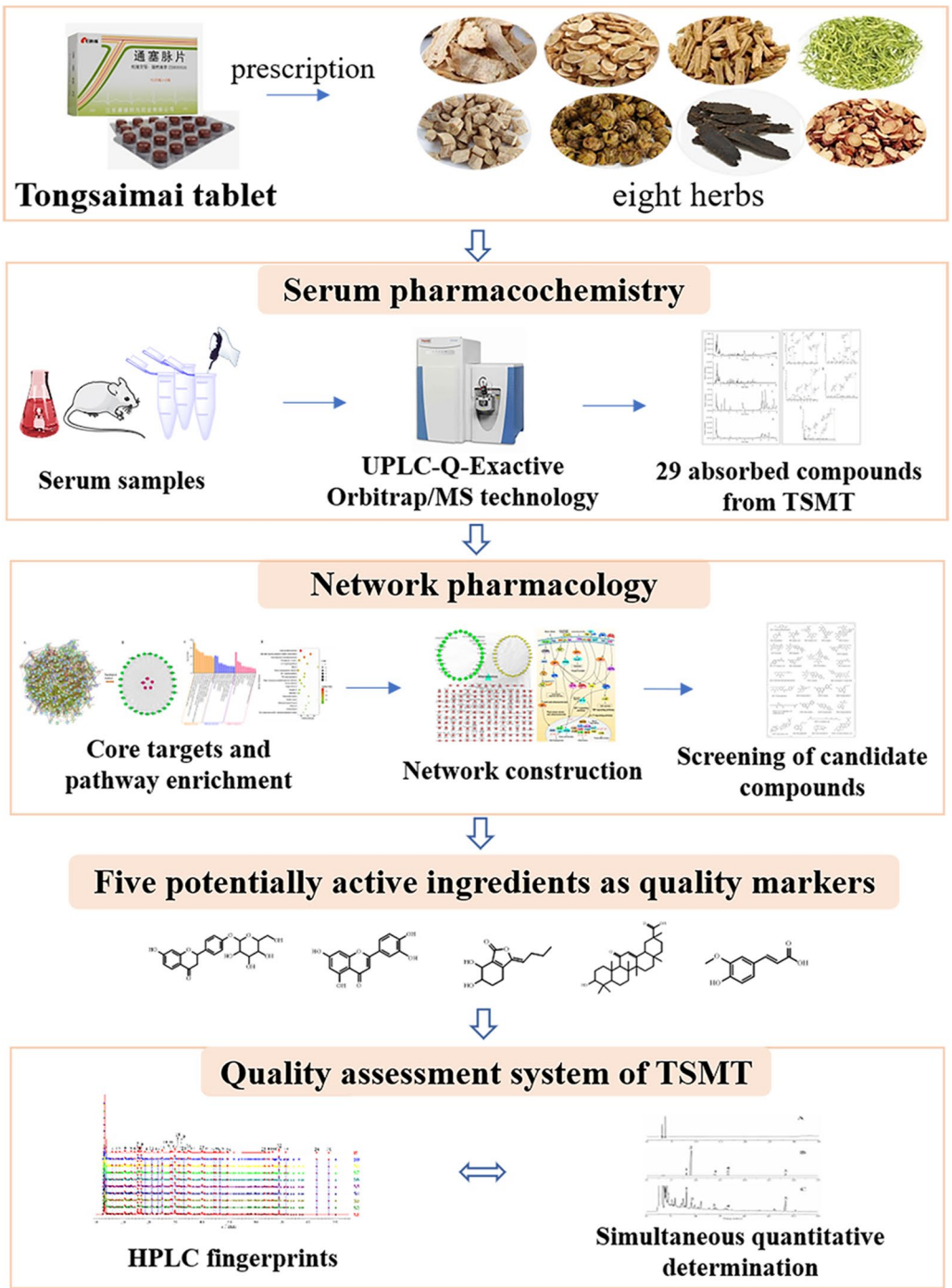

Fig. 1 Schematic diagram exploring the quality assessment of Tongsaimai tablets by integrating serum pharmacochemistry and network pharmacology

standards including Ferulic acid, Liquiritin, Senkyunolide I, Luteolin, and Glycyrrhizic acid, at the concentration of 84.60, 360.00, 132.40, 112.40, 221.60 mg/L, respectively. It was generated six different concentration gradients for HPLC fingerprint and content determination analysis. All standard solutions were stored at 4 °C before use.

Approximately 0.35 g of TSMT samples were fully ground, and diluted in 10 mL of 70% methanol (v/v) for

45 min using ultrasonication. Finally, the TSMT samples from each batch were filtered through a 0.22 μm membrane filter after centrifugation at 10,000 rpm for 10 min. All TSMT sample solutions were stored at 4 °C before performing UPLC-QTOF-MS analysis, followed by determination and fingerprint analysis.

Preparation of serum samples from mice administrated with TSMT

Male BALB/c mice (aged 4–6 weeks and weighting 16 ~ 18 g, certificate number: SCXK (Beijing) 2019–0010) were obtained from SPF Biotechnology Co., Ltd. (Beijing, China). All animals were kept at 12 h light/dark cycle at the animal care facility under standard conditions. The animals were acclimatized for at least 7 days before the start of the experiment, and were fed a fresh diet with free access to water. The animal experiments were approved by the ethics committee of the Chengdu University of Traditional Chinese Medicine (CDUTCM, permit CDU2020KB097), and were conducted in strict accordance with the Guidelines for the Care and Use of Laboratory Animals of the Ministry of Science and Technology of China.

For serum pharmacochemistry study, mice were orally administered with 0.6825 g/kg of TSMT solution, while sterile saline was used as the blank group. After 1 h of oral administration via the retroorbital sinus, blood samples (500 μL) were collected and centrifuged at 3500 rpm for 15 min. Next, 600 μL of acetonitrile was added to 200 μL of serum samples, vortexed, and centrifuged at 12,000 rpm for 10 min for protein-precipitation. The obtained supernatant was dried using nitrogen gas. The precipitate was redissolved in a 1 mL mobile phase, followed by swirling and centrifugation at 12,000 rpm for 15 min. Finally, the collected supernatant was used to perform UPLC-Q-Exactive Orbitrap/MS analysis.

UPLC-Q-exactive orbitrap/MS analysis

Dionex UltiMate 3000 Rapid Separation UPLC system (Thermo Fisher Scientific Inc., USA) equipped with a DAD-3000RS detector was used to carry out the chromatographic analysis. The chromatographic separation was performed on an Accucore™ C18 column (100 × 2.1 mm, 2.6 μm, Thermo Fisher Scientific Inc., USA) at 30 °C. The mobile phases were composed of 0.1% formic acid in water (A) and acetonitrile (B) (v/v) with a flow rate of 0.30 mL/min and an injection volume of 2 μL. The gradient elution program was as follows: 0 ~ 10 min 5 ~ 20% B, 10 ~ 25 min 20% ~ 60% B, 25 ~ 40 min 60% ~ 95% B. The online UV spectra were recorded in the range of 190 ~ 400 nm.

To identify chemical compounds in both TSMT samples and serum samples of mice administered with TSMT, we used ultra-performance liquid chromatography Q-Exactive Orbitrap tandem mass spectrometry (UPLC-Q-Exactive Orbitrap/MS) (Thermo Fisher Scientific Inc., USA) fitted with electrospray ionization (ESI) source, where the following experimental parameters setting were used: ion spray voltage, 3 kV; collision energy, 35 eV; capillary voltage,4 kV; capillary temperature, 320 °C; heater temperature, 300 °C; sheath gas flow rate, 35 Arb; auxiliary gas flow rate, 10 Arb. Both positive and negative ion modes were performed on the instrument with the full scan range of 50–1500 m/z. Data were processed and analyzed using Xcalibur™ version2.2.1 and Trace Finder3.3 version (Thermo Fisher Scientific Inc, USA) along with compound discoverer 3.0 software (Thermo Fisher Scientific Inc., USA). Molecular qualitative analysis of all samples was measured in contrast with retention times and MS spectra through available reference standards.

Network pharmacology analysis

The structural formulas (*.sdf / SMILES) of potential active components were identified using UPLC-Q-Exactive Orbitrap/MS, which were determined and downloaded from ChemSpider (http://www.chemspider.com/) and PubChem (https://pubchem.ncbi.nlm.nih.gov/) and drawn using Chemdraw 18.0 software. Next, all predicted targets of components were obtained from Swiss Target Prediction (http://www.swisstargetprediction.ch/) to perform reverse docking based on structural similarity. Additionally, GeneCards (https://www.genecards.org/) was used to obtain the targets closely related to AS. All the target names were standardized into official gene symbols (Homo sapiens) using the UniProt database (http://www.uniprot.org/). Finally, the intersecting targets overlapping the TSMT compound targets and AS-related genes were obtained.

To filter out and select functional core targets, we constructed the protein–protein interaction (PPI, p-value < 0.01) for the intersection targets between TSMT compounds and AS disease using the STRING database (https://string-db.org/), where "homo sapiens" species was selected. The PPI network from the STRING database was then imported into Cytoscape 3.7.1 software to construct target network. Meanwhile, the analyzer plugin of Cytoscape 3.7.1 was used to calculate all nodes with the topological property of Betweenness, Closeness, and degree centrality representing predicted targets in the network. Finally, the candidate hub targets were screened at degree values higher than 99.

To further characterize the functional meaning and explain the biological roles of the above confirmed key targets, the Discovery database (DAVID 6.8, https://david.ncifcrf.gov/home.jsp) was used for performing

Gene ontology (GO) analysis including biological processes, cellular components, and molecular function. Further, to perform target annotation, visualization, and integration (P-value < 0.01), the enrichment pathway analysis was carried out based on Kyoto Encyclopedia of Genes and Genomes database (KEGG, http://www.genome.jp/kegg/). As a result, a "component-targets-pathway-disease" network was constructed by means of Cytoscape 3.7.1 software to reveal the underlying mechanism of the disease. Moreover, Additionally, R 4.0.3 software was used to draw the bubble map to visualize the results of the pathway annotation. Therefore, initially, we selected the above active compositions related closely to AS targets as candidates for establishing a quality assessment system for TSMT.

Determination of five markers of TSMT

HPLC instrumentation and conditions

Quantitative analysis and fingerprint analysis were performed using UltiMate 3000 HPLC instrument (ThermoFisher, USA) with a DAD 3000 detector, a ternary pump of SR3000 Solvent Rack, a WPS-3000SL autosampler, a TCC-3000SD column temperature controller, and a workstation of Chromeleon 7.2. The compounds separation was performed on a Thermo Hypersil Gold C18 column (250 mm × 4.6 mm, 5 μm). The mobile phase consisted of 0.1% phosphoric acid (solvent A) and Acetonitrile (solvent B) at a flow rate of 1 mL/min, which followed a gradient program of 0–20 min, 18–35% B; 20–30 min, 35–48% B; 30–35 min. The column temperature was maintained at 30 °C while the autosampler temperature was maintained at 4 °C with 10 μL of sample solution being injected. Both the detection wavelength of DAD was monitored at 235 nm.

Validation of the method

According to the recommendations and guidelines of *Chinese Pharmacopoeia*, the validation of the HPLC content determination method included calibration curves, precision, stability, repeatability, and recovery tests. Among these, we established the calibration curves by analyzing the mixed standard solutions containing five reference substances at six concentration levels. These curves were drawn by plotting the relationship between different peak areas (y) and the corresponding concentration (x, mg/L) of analytes with least-square linear regression to conduct calibration curves. For confirmatory methods, the correlation coefficient (r) of linear regression equations should not be lower than 0.999. The precision was measured by conducting six consecutive analyses of one sample solution. The repeatability was assessed by analyzing six parallel sample solutions prepared from the same batch. The stability was estimated using replicates of one sample solution at different time points (0, 2, 4, 8, 12, 24 h). To determine the precision, stability, and repeatability of the test solution, Relative Standard Deviation (RSD%) was calculated. Finally, the recovery test, i.e., adding reference standards of corresponding compounds at certain levels into the above sample solutions, was performed by analyzing six parallel solutions from the same batch. Thus, the accuracy of the method was confirmed. Additionally, to evaluate the average recovery of analytes, the corresponding peak areas were measured and analyzed.

Determination of the contents

Sample solutions for five potentially effective compounds in nine batches of TSMT were prepared using the above-mentioned method. Of which, 10 μL was injected under HPLC conditions to measure the peak area of each compound and calculate all TSMT contents. However, the content determination limit needs further verification to exhibit better control over the quality of the TSMT preparation.

HPLC fingerprint analysis

HPLC conditions

The chromatographic conditions for fingerprint analysis were the same as mentioned for quantitative analysis, except, the gradient elution for the chemical fingerprint was as follows: 0–25 min, 5–17% B; 25–50 min, 17–25% B; 50–80 min, 25–55% B; 80–95 min, 55–95%.

Validation of the methods

The validation of fingerprint method including repeatability, precision, and stability tests were also measured using the above-mentioned method. A reference peak was set as per the chemical profiles and characteristics of fingerprints, after which relative peak areas (RPA) of common peaks (the peak areas > 0.2) were used to detect and evaluate the fingerprint. RSD% was calculated and evaluated the results of RPA for the precision, stability, and repeatability of the test solution.

Similarity analysis

Based on the fingerprint chromatographic conditions for the fingerprint method, each chromatogram file of nine detected samples of TSMT was derived with "*.cdf" format using Chromeleon 7.2 workstation. It was then manipulated by a professional software called Similarity Evaluation System for Chromatographic Fingerprint of Traditional Chinese Medicine, provided by the Chinese Pharmacopoeia Committee (Version 2012A) (Beijing, China). This calculated and generated simulated reference fingerprints, while separately counted separately

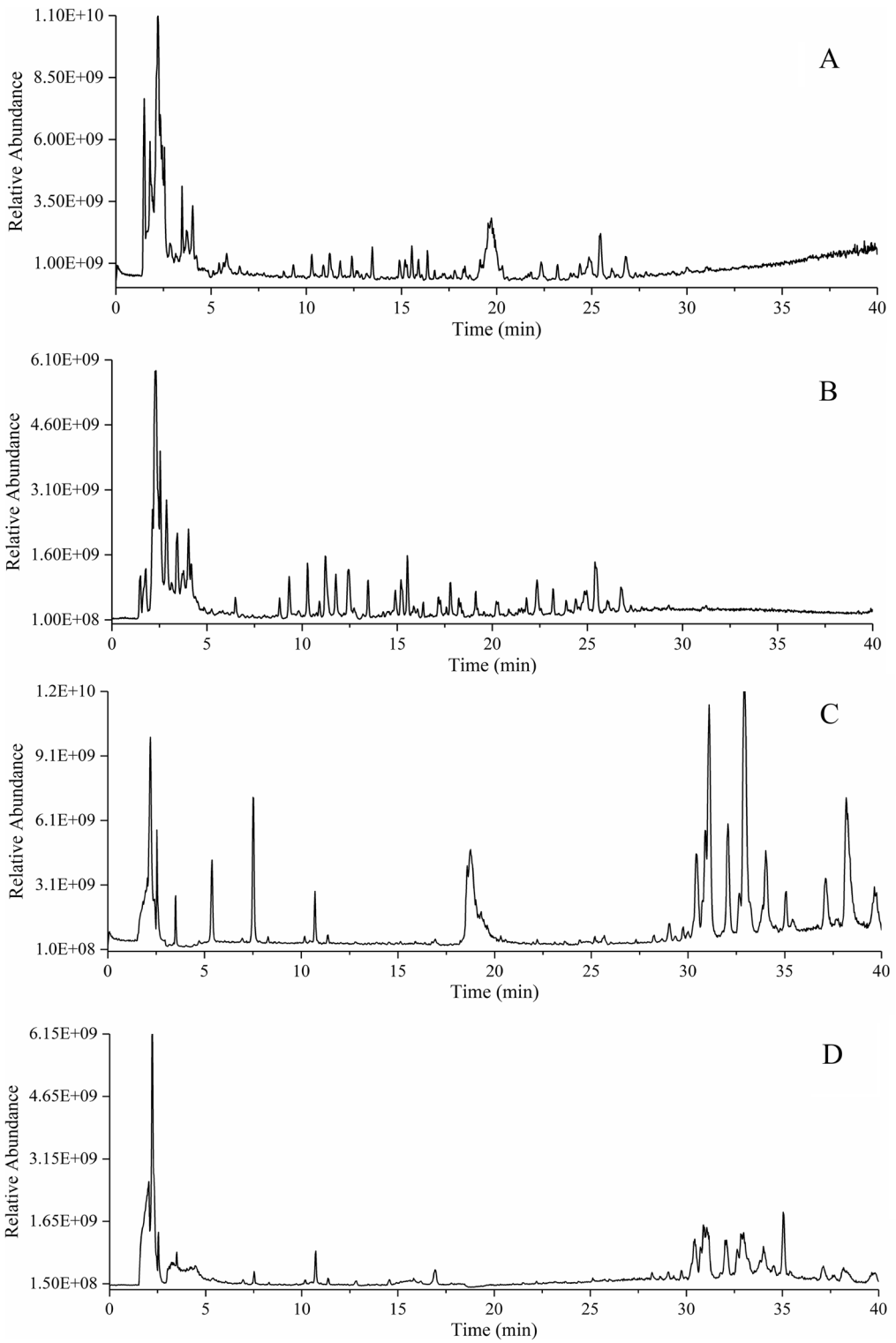

Fig. 2 Base peak chromatograms of TSMT samples by UPLC-Q-Exactive Orbitrap/MS in positive (**A**) and negative modes (**B**), and base peak chromatograms of TSMT-derived serum in positive (**C**) and negative modes (**D**)

Table 1 Identification results of all constituents of TSMT in vitro and in vivo by UPLC-Q-exactive MS/MS via MS data in (+/−) ESI modes

Peak no	tR/min	Name	Formula	Mass ion type	Mean measured	Theoretical exact	Mass error(ppm)	Fragment ions	References
1	2.28	5-Hydroxymethyl-furfural [M]	$C_6H_6O_3$	$[M+H]^+$	127.0389	127.0390	− 0.79	127.0389, 109.0286, 81.0340	[15, 37]
2	2.39	Achyranthine [M]	$C_6H_{11}NO_2$	$[M+H]^+$	130.0862	130.0863	− 0.77	130.0862, 112.0760, 84.0812	[37]
3	2.90	Quinic acid [M]	$C_7H_{12}O_6$	$[M-H]^-$	191.0555	191.0561	− 3.14	191.0555, 173.0444, 127.0391, 85.0284	[38]
4	3.32	Codonopsinol A	$C_{13}H_{19}NO_5$	$[M+H]^+$	270.1331	270.1336	− 1.85	270.1331, 74.0606	[39]
5	3.42	Codonopsinol	$C_{14}H_{21}NO_5$	$[M+H]^+$	284.1488	284.1492	− 1.41	284.1488, 88.0761	[39]
6	3.63	codonopiloside A	$C_{19}H_{29}NO_9$	$[M+H]^+$	416.1917	416.1915	0.48	416.1917, 254.1384, 236.1097, 187.0753, 161.0597	[39]
7	4.03	Codonopsinol B	$C_{13}H_{19}NO_4$	$[M+H]^+$	254.1387	254.1387	0.00	254.1387, 236.1286, 161.0594	[39]
8	4.24	Codonopsine	$C_{14}H_{21}NO_4$	$[M+H]^+$	268.1541	268.1543	− 0.75	268.1541, 88.0761	[40]
9	5.71	Gallic acid [#]	$C_7H_6O_5$	$[M-H]^-$	169.0134	169.0142	− 4.73	169.0134, 125.0235	[38]
10	6.49	Harpagide [#]	$C_{15}H_{24}O_{10}$	$[M-H]^-$	363.1292	363.1297	− 1.38	363.1292, 201.0763, 183.0656, 165.0548, 139.0931	[41]
11	6.92	3,4-dihydroaucubin	$C_{15}H_{24}O_9$	[M+COOH]−	393.1398	393.1402	− 1.02	393.1398, 347.1346, 239.4955, 167.0707,127.0392	[42]
12	7.10	Woodorien	$C_{14}H_{18}O_9$	$[M-H]^-$	329.0890	329.0878	3.65	329.0890, 167.0342, 152.0107, 123.0441, 108.0207	[40]
13	7.61	Danshensu	$C_9H_{10}O_5$	$[M-H]^-$	197.0448	197.0455	− 3.55	197.0448, 179.0342, 152.9037, 135.0442, 123.0442	[43]
14	7.73	Vanilloside	$C_{14}H_{18}O_8$	[M+COOH]−	359.0985	359.0984	0.28	359.0985, 313.0928, 197.0449, 161.0448, 151.0392	[44]
15	8.09	Decaffeoylacteo-side	$C_{20}H_{30}O_{12}$	$[M-H]^-$	461.1667	461.1664	0.65	461.1667, 315.1097, 161.0446, 135.0443,113.0235	[41]
16	8.12	8-epi-Loganic acid	$C_{16}H_{24}O_{10}$	$[M-H]^-$	375.1292	375.1297	− 1.33	375.1290, 213.0763, 169.0863, 151.0760, 113.0235	[38]
17	8.86	Loganic acid [M]	$C_{16}H_{24}O_{10}$	$[M-H]^-$	375.1290	375.1297	− 1.87	375.1290, 213.0763, 169.0863, 151.0760, 113.0235	[38]
18	8.88	Isoferulic acid	$C_{10}H_{10}O_4$	$[M+H]^+$	195.0647	195.0652	− 2.56	195.0647, 177.0545, 149.0596	[15, 39, 43, 45]
19	9.24	Caffeic acid	$C_9H_8O_4$	$[M+H]^+$	181.0499	181.0495	2.21	181.0499, 163.0388, 135.0440, 89.0390	[46, 47]
20	9.31	Chlorogenic acid isomer	$C_{16}H_{18}O_9$	$[M-H]^-$	353.0878	353.0878	0.00	353.0878, 191.0555, 179.0343, 161.0235, 135.0443	[47]
21	10.09	Tangshenoside II	$C_{17}H_{24}O_9$	$[M-H]^-$	371.1343	371.1348	− 1.35	371.1343, 209.0645, 191.0906	[40]
22	10.10	Methyl caffeate	$C_{10}H_{10}O_4$	$[M+H]^+$	195.0652	195.0652	0.00	195.0652, 163.0656, 133.0284	[38]
23	10.21	Quercetin di-O-glucoside	$C_{27}H_{30}O_{17}$	$[M-H]^-$	625.1404	625.1410	− 0.96	625.1404, 463.0866, 299.0197, 151.0029	[42]
24	10.29	Aucubin	C15H22O9	$[M-H]^-$	345.1191	345.1191	0.00	345.1191, 183.0659, 165.0550, 139.0753, 121.0649	[41]
25	10.31	Secologanoside	$C_{16}H_{22}O_{11}$	$[M-H]^-$	389.1086	389.1089	− 0.77	389.1086, 345.1182, 209.0451, 183.0658,165.0547, 121.0649	[41]
26	10.74	Secologanic acid or isomer	$C_{16}H_{22}O_{10}$	$[M-H]^-$	373.1143	373.1140	0.80	373.1143, 211.0606, 193.0500, 149.0596, 123.0446	[41]
27	10.96	Liquiritigenin 4′,7-diglucoside isomer	$C_{27}H_{32}O_{14}$	$[M-H]^-$	579.1699	579.1719	− 3.45	579.1699, 255.0660, 153.0184, 119.0492	[41]
28	11.23	Chlorogenic acid [#]	$C_{16}H_{18}O_9$	$[M-H]^-$	353.0878	353.0878	0.00	353.0878, 191.0555, 179.0343, 163.0388, 161.0235, 135.0440	[47]
29	11.59	Cistanoside F	$C_{21}H_{28}O_{13}$	$[M-H]^-$	487.1453	487.1457	− 0.82	487.1453, 307.0816, 163.0392, 145.0287	[48]
30	11.68	Loganin [M]	$C_{17}H_{26}O_{10}$	$[M-H]^-$	435.1505	435.1508	− 0.69	435.1505, 227.0923, 210.0761, 127.0391, 101.0234	[41]
31	11.77	Neochlorogenic acid	$C_{16}H_{18}O_9$	$[M-H]^-$	353.0877	353.0878	− 0.28	353.0877, 191.0555, 179.0448, 161.0236, 135.0442	[47]
32	12.05	Vicenin-2 [M]	$C_{27}H_{30}O_{15}$	$[M-H]^-$	593.1499	593.1512	− 2.19	593.1499, 503.1164, 473.1091, 383.0769, 353.0666	[45]

Table 1 (continued)

Peak no	tR/min	Name	Formula	Mass ion type	Mean measured	Theoretical exact	Mass error(ppm)	Fragment ions	References
33	12.06	3-Feruloylquinic acid	$C_{17}H_{20}O_9$	$[M-H]^-$	367.1038	367.1035	0.82	367.1038, 193.0500, 173.0444, 134.0364	[41]
34	12.40	Sweroside [M]	$C_{16}H_{22}O_9$	$[M+H]^+$	359.1329	359.1337	− 2.23	359.1329, 197.0807, 127.0390	[41]
35	12.76	Aucubin isomer	$C_{15}H_{22}O_9$	$[M-H]^-$	345.1187	345.1191	− 1.16	345.1187, 183.0657, 165.0549, 139.0757, 121.0648	[41]
36	13.28	Schaftoside	$C_{26}H_{28}O_{14}$	$[M-H]^-$	563.1401	563.1406	− 0.89	563.1401, 545.1277, 503.1202, 473.1082, 443.0988, 353.0663	[14, 18, 45]
37	13.44	Benzoic acid	$C_7H_6O_2$	$[M+H]^+$	123.0442	123.0441	0.81	123.0442, 95.0495, 79.0184	[15]
38	13.48	Kingiside [M]	$C_{17}H_{24}O_{11}$	$[M-H]^-$	403.1250	403.1246	0.99	403.1250, 371.0981, 223.0604, 179.0555, 165.0550, 121.0285	[41]
39	13.79	Schaftoside isomer	$C_{26}H_{28}O_{14}$	$[M-H]^-$	563.1401	563.1406	− 0.89	563.1401, 503.1207, 473.1065, 443.0972, 353.0665	[14, 18, 45]
40	14.02	Caffeic acid hexoside	$C_{16}H_{22}O_8$	$[M-H]^-$	341.1238	341.1242	− 1.17	341.1238, 179.0708, 161.0600	[38]
41	14.26	(E)-2-Hexenyl-a-L arabinopyrano-syl- (1/2)-b-D glucopyranoside	$C_{17}H_{30}O_{10}$	$[M-H]^-$	393.1756	393.1766	− 2.54	393.1756, 261.1332, 179.0554, 149.0448	[40]
42	14.33	5-Feruloylquinic acid	$C_{17}H_{20}O_9$	$[M-H]^-$	367.1022	367.1035	− 3.54	367.1022, 193.0554, 173.0447, 134.0363	[41]
43	14.44	Isoviolanthin	$C_{27}H_{30}O_{14}$	$[M-H]^-$	577.1556	577.1563	− 1.21	577.1556, 269.0454	[45]
44	14.61	6-O-Methylaucubin	$C_{16}H_{24}O_9$	$[M-H]^-$	359.1342	359.1348	− 1.67	359.1342, 197.0813, 153.0911	[42]
45	14.71	Apigenin-6,8-di-C-β-D-xyloside	$C_{25}H_{26}O_{13}$	$[M-H]^-$	533.1293	533.1301	− 1.50	533.1293, 515.1181, 473.1078, 443.0986, 383.0771, 353.0606, 297.0768, 135.0442	[49]
46	14.79	Hexyl β-sophoroside	$C_{18}H_{34}O_{11}$	$[M-H]^-$	425.2025	425.2028	− 0.71	425.2025, 263.1495, 161.0447	[50]
47	14.85	β-Ecdysone[#]	$C_{27}H_{44}O_7$	$[M+H]^+$	481.3151	481.3160	− 1.87	481.3151, 445.2942, 371.2211, 165.1273	[38]
48	14.91	Rutin	$C_{27}H_{30}O_{16}$	$[M-H]^-$	609.1454	609.1461	− 1.15	609.1456, 300.0272, 271.0246, 255.0295, 243.0294, 151.0028	[38, 45]
49	14.94	Calycosin-7-O-β-D-glucoside[#]	$C_{22}H_{22}O_{10}$	$[M+H]^+$	447.1287	447.1286	0.22	447.1287, 283.0610, 268.0375, 239.0346, 211.0394	[50]
50	14.94	Lonicerin	$C_{27}H_{30}O_{15}$	$[M-H]^-$	593.1506	593.1512	− 1.01	593.1506, 285.0403	[39]
51	14.98	20,26-dihydroxy-ecdysone	$C_{27}H_{44}O_8$	$[M+COOH]-$	541.3009	541.3018	− 1.66	541.3009, 495.2962, 477.2855, 335.1869	[37]
52	15.12	Vitexin	$C_{21}H_{20}O_{10}$	$[M+H]^+$	433.1124	433.1129	− 1.15	433.1124, 313.0701, 283.0599	[45]
53	15.18	Acteoside [#]	$C_{29}H_{36}O_{15}$	$[M-H]^-$	623.1976	623.1981	− 0.80	623.1976, 461.1656, 315.1098, 179.0345, 161.0236, 113.0286	[41]
54	15.23	Isoliquiritin	$C_{21}H_{22}O_9$	$[M-H]^-$	417.1188	417.1191	− 0.72	417.1188, 255.0660, 135.0078, 119.0493	[18]
55	15.24	Liquiritigenin [M]	$C_{15}H_{12}O_4$	$[M+H]^+$	257.0804	257.0808	− 1.56	257.0804, 239.0702, 147.0439, 137.0232	[18]
56	15.25	Isoliquiritin apioside	$C_{26}H_{30}O_{13}$	$[M-H]^-$	549.1608	549.1614	− 1.09	549.1608, 255.0660, 135.0078, 119.0492	[41]
57	15.27	Nicotiflorin or isomer [M]	$C_{27}H_{30}O_{15}$	$[M-H]^-$	593.1507	593.1512	− 0.84	593.1507, 447.0921, 285.0403, 151.0029	[41]
58	15.31	Liquiritigenin 4′,7-diglucoside	$C_{27}H_{32}O_{14}$	$[M-H]^-$	579.1699	579.1719	− 3.45	579.1699, 255.0660, 153.0184, 119.0492	[41]
59	15.31	5-Hydroxyliquiritin	$C_{21}H_{22}O_{10}$	$[M-H]^-$	433.1130	433.1140	− 2.31	433.1130, 271.0610, 151.00328	[14]
60	15.32	Naringenin or isomer	$C_{15}H_{12}O_5$	$[M+H]^+$	273.0753	273.0757	− 1.46	273.0753, 153.0181, 147.0439, 119.0492	[41, 44]
61	15.42	Senkyunolide H	$C_{12}H_{16}O_4$	$[M+H]^+$	225.1131	225.1121	4.44	225.1131, 207.1014, 165.0909, 161.0958	[16]
62	15.52	Tangshenoside V isomer	$C_{21}H_{26}O_{12}$	$[M-H]^-$	469.1346	469.1351	− 1.07	469.1336, 325.0927, 265.0715, 235.0607, 163.0393, 19.0493	[50]
63	15.58	Cynaroside [#]	$C_{21}H_{20}O_{11}$	$[M-H]^-$	447.0929	447.0933	− 0.89	447.0929, 285.0403	[38]
64	15.58	Quercetin	$C_{15}H_{10}O_7$	$[M+H]^+$	303.0494	303.0499	− 1.65	303.0494, 285.0393, 257.0441, 229.0495, 153.0181	[46]

Table 1 (continued)

Peak no	tR/min	Name	Formula	Mass ion type	Mean measured	Theoretical exact	Mass error(ppm)	Fragment ions	References
65	15.58	Hyperoside	$C_{21}H_{20}O_{12}$	$[M-H]^-$	463.0880	463.0882	− 0.43	463.0880, 300.0273, 271.0247, 255.0297	[41]
66	15.60	Lobetyolinin	$C_{26}H_{38}O_{13}$	[M + COOH]−	603.2290	603.2294	− 0.66	603.2290, 323.0977, 221.0661, 179.0554	[39]
67	15.60	p-Coumaric acid [M]	$C_9H_8O_3$	$[M-H]^-$	163.0394	163.0401	− 4.29	163.0394, 119.0494	[41, 44, 50]
68	15.63	Liquiritin [M]	$C_{21}H_{22}O_9$	$[M-H]^-$	417.1187	417.1191	− 0.96	417.1187, 255.0660, 135.0078, 119.0493, 91.0179	[18]
69	15.74	Sibirioside A	$C_{21}H_{28}O_{12}$	[M + COOH]−	517.1558	517.1563	− 0.97	517.1558,471.1507, 323.0979, 189.0550, 161.0598, 147.0443	[41]
70	15.84	Isoacteoside	$C_{29}H_{36}O_{15}$	$[M-H]^-$	623.1978	623.1981	− 0.48	623.1978, 461.1673, 315.1076, 179.0343, 161.0236	[41]
71	15.94	Hexyl-(pen)-glucoside	$C_{17}H_{32}O_{10}$	[M + COOH]−	441.1977	441.1978	− 0.23	441.1977, 395. 1919, 263.1497, 161.0446	[50]
72	16.02	Vallinic acid	$C_8H_8O_4$	$[M-H]^-$	167.0342	167.0350	− 4.79	167.0342, 123.0442	[14, 40, 41, 45, 46]
73	16.06	Naringin	$C_{27}H_{32}O_{14}$	$[M-H]^-$	579.1722	579.1719	0.52	579.1722, 417.1551, 387.1083, 181.0499, 166.0264	[49]
74	16.28	Angoroside C	$C_{36}H_{48}O_{19}$	$[M-H]^-$	783.2706	783.2717	− 1.40	783.2701, 607.2206, 193.0507, 175.0393, 160.0158	[41]
75	16.32	Violanthin	$C_{27}H_{30}O_{14}$	$[M-H]^-$	577.1558	577.1563	− 0.87	577.1558, 503.1201, 457.1105, 383.0772	[45]
76	16.33	Morroniside	$C_{17}H_{26}O_{11}$	$[M-H]^-$	405.1403	405.1402	0.25	405.1403, 243.1232, 225.1115, 101.0235	[41]
77	16.39	Ferulic acid [#M]	$C_{10}H_{10}O_4$	$[M+H]^+$	195.0660	195.0652	4.10	195.0660, 177.0544, 149.0595, 145.0283, 117.0336	[15, 39, 43, 45]
78	16.48	Iso-angoroside C	$C_{36}H_{48}O_{19}$	$[M-H]^-$	783.2701	783.2717	− 2.04	783.2706, 607.2253, 193.0499, 175.0393, 160.0158	[41]
79	16.50	3-Hexenyl-β-D-glucopyranoside [M]	$C_{12}H_{22}O_6$	$[M-H]^-$	261.1340	261.1344	− 1.53	262.1340, 187.0969, 125.0962	[50]
80	16.55	Astragalin	$C_{21}H_{20}O_{11}$	$[M-H]^-$	447.0928	447.0933	− 1.12	447.0928, 284.0324, 255.0295, 227.0345	[38]
81	16.67	isorhamnetin-3-O-glucoside	$C_{22}H_{22}O_{12}$	$[M+H]^+$	479.1189	479.1184	1.04	479.1189, 317.0652, 302.0414, 274.0465, 153.0179	[46]
82	16.79	Lobetyol	$C_{14}H_{18}O_3$	[M + COOH]−	279.1236	279.1238	− 0.72	279.1236, 235.1335, 205.1227, 137.0755	[51]
83	16.84	Genistin [M]	$C_{21}H_{20}O_{10}$	$[M+H]^+$	433.1122	433.1129	− 1.62	433.1122, 271.0596, 243.0651, 153.0180	[46]
84	16.96	Tangshenoside V	$C_{21}H_{26}O_{12}$	$[M-H]^-$	469.1334	469.1351	− 3.62	469.1334, 367.1006, 325.0924, 271.0605, 163.0392, 119.0492	[50]
85	17.00	Naringenin-6-C-glucoside	$C_{21}H_{22}O_{10}$	$[M-H]^-$	433.1133	433.1140	− 1.62	433.1133, 271.0601, 151.0028, 119.0493	[41]
86	17.05	6-Methoxyluteolin 3′-Glucoside	$C_{22}H_{22}O_{11}$	$[M-H]^-$	461.1083	461.1089	− 1.30	461.1083, 283.0245, 255.0295	[41]
87	17.22	3,5-O-Dicaffeoyl quinic acid	$C_{25}H_{24}O_{12}$	$[M-H]^-$	515.1189	515.1195	− 1.16	515.1189, 353.0875, 191.0554, 179.0342, 135.0442	[47]
88	17.26	Naringenin 4′-O-glucoside	$C_{21}H_{22}O_{10}$	$[M-H]^-$	433.1131	433.1140	− 2.08	433.1131, 271.0610, 151.0028, 119.0493	[41]
89	17.27	Scrophulide	$C_{30}H_{38}O_{15}$	$[M-H]^-$	637.2131	637.2138	− 1.10	637.2131, 161.0236	[42]
90	17.36	Genistein	$C_{15}H_{10}O_5$	$[M-H]^-$	269.0453	269.0455	− 0.74	269.0453,255.0603, 225.0553, 153.0184, 133.0285	[46]
91	17.37	Rhamnocitrin	$C_{16}H_{12}O_6$	$[M+H]^+$	301.0702	301.0707	− 1.66	301.0702, 245.0801, 231.06549, 167.0336	[14, 41]
92	17.49	Lobetyolin	$C_{20}H_{28}O_8$	[M + COOH]−	441.1764	441.1766	− 0.45	441.1764, 279.0669, 215.1068, 185.096	[39]
93	17.51	Liquirtin apioside	$C_{26}H_{30}O_{13}$	$[M-H]^-$	549.1606	549.1614	− 1.46	549.1606, 417.1208, 255.0659, 153.0184, 119.0492	[41]
94	17.83	4,5-O-Dicaffeoyl quinic acid	$C_{25}H_{24}O_{12}$	$[M-H]^-$	515.1200	515.1195	0.97	515.1200, 353.0875, 191.0555, 173.0447	[47]
95	17.85	3-Butyl-4-hydroxyphthalide	$C_{12}H_{14}O_3$	[M + H]−	207.1014	207.1016	− 0.97	207.1014, 189.0909, 161.0960	[16]

Table 1 (continued)

Peak no	tR/min	Name	Formula	Mass ion type	Mean measured	Theoretical exact	Mass error(ppm)	Fragment ions	References
96	18.17	Naringenin 7-O-glucoside [M]	$C_{21}H_{22}O_{10}$	$[M-H]^-$	433.1123	433.1140	− 3.93	433.1123, 271.0611, 151.0028, 119.0492	[41]
97	18.18	Naringenin	$C_{15}H_{12}O_5$	$[M+H]^+$	273.0753	273.0757	− 1.46	273.0753, 153.0181, 147.0439, 119.0492	[41, 44]
98	18.32	Neoisoliquiritin [M]	$C_{21}H_{22}O_9$	$[M-H]^-$	417.1189	417.1191	− 0.48	417.1189, 255.0660, 135.0078	[18]
99	18.40	Z-harpagoside	$C_{24}H_{30}O_{11}$	$[M-H]^-$	493.1709	493.1715	− 1.22	493.1709, 345.1181, 183.0656, 147.0443	[41]
100	18.41	Ononin	$C_{22}H_{22}O_9$	$[M+H]^+$	431.1335	431.1337	− 0.46	431. 1335, 269. 0806, 254.0573, 213.0912, 118.0416	[14]
101	18.54	Senkyunolide I [# M]	$C_{12}H_{16}O_4$	$[M+H]^+$	225.1119	225.1121	− 0.89	225.1119, 207.1013, 189.0906, 179.1059, 161.0958	[16]
102	18.63	Cistanoside D	$C_{31}H_{40}O_{15}$	$[M-H]^-$	651.2281	651.2294	− 2.00	652.2371, 193.0502, 175.0394	[42]
103	19.01	Harpagoside [#]	$C_{24}H_{30}O_{11}$	$[M-H]^-$	493.1703	493.1715	− 2.43	493.1703, 345.1181, 183.0656, 147.0443	[41]
104	19.15	Senkyunolide F	$C_{12}H_{14}O_3$	$[M+H]^+$	207.1013	207.1016	− 1.45	207.1013, 189.0907, 161.0962	[16]
105	19.16	Astragaloside VII isomer	$C_{47}H_{78}O_{19}$	$[M+COOH]-$	991.5122	991.5119	0.30	991.5122, 945.5055, 783.4508	[41]
106	19.36	Isomucronulatol 7-O-glucoside	$C_{23}H_{28}O_{10}$	$[M-H]^-$	463.1616	463.1610	1.30	463.1616, 301.1078, 286.0844, 179.0706,135.0442	[52]
107	19.46	Licochalcone B	$C_{16}H_{14}O_5$	$[M-H]^-$	285.0764	285.0768	− 1.40	285.0764, 270.0530, 177.0183, 150.0313	[18]
108	19.50	Emodin	$C_{15}H_{10}O_5$	$[M-H]^-$	269.0453	269.0455	− 0.74	269.0453, 241.0504, 213.0547	[40, 43]
109	19.55	Baicalin	$C_{21}H_{18}O_{11}$	$[M-H]^-$	445.0770	445.0776	− 1.35	445. 0770, 269. 0454, 251. 0340, 223. 0394	[46]
110	19.92	6-Methoxyluteolin 7-Glucoside	$C_{22}H_{22}O_{11}$	$[M-H]^-$	461.1080	461.1089	− 1.95	461.1080, 299.0558, 283.0245, 255.0295	[41]
111	20.12	Coumarin	$C_9H_6O_2$	$[M+H]^+$	147.0438	147.0441	− 2.04	147.0438, 119.0548	[46]
112	20.30	Isoliquiritigenin	$C_{15}H_{12}O_4$	$[M+H]^+$	257.0804	257.0808	− 1.56	257.0804, 239.0701, 147.0439, 137.0232, 119.0492	[18]
113	20.30	Calycosin	$C_{16}H_{12}O_5$	$[M-H]^-$	283.0609	283.0612	− 1.06	283.0609, 268.0374, 223.0397, 148.0158, 135.0081	[18, 41]
114	20.40	Luteolin [# M]	$C_{15}H_{10}O_6$	$[M+H]^+$	287.0544	287.0550	− 2.09	287.0544, 153.0180, 135.0439	[38, 43]
115	20.46	Licoricesaponin G2 or isomer	$C_{42}H_{62}O_{17}$	$[M+H]^+$	839.4050	839.4060	− 1.19	839.4050, 469.3307	[14]
116	20.73	Astragaloside VII	$C_{47}H_{78}O_{19}$	$[M+COOH]-$	991.5122	991.5119	0.30	991.5122, 945.5055, 783.4508	[41]
117	21.02	senkyunolide C [M]	$C_{12}H_{12}O_3$	$[M+H]^+$	205.0855	205.0859	− 1.95	205.0855, 187.0752, 149.0232	[16]
118	21.24	2-Hydroxyethyl 4-methoxycinnamate	$C_{12}H_{14}O_4$	$[M-H]^-$	221.0812	221.0819	− 3.17	221.0812, 177.0913	[42]
119	21.35	Cnidilide	$C_{12}H_{18}O_2$	$[M+H]^+$	195.1378	195.1380	− 1.02	195.1378, 177.1271, 149.1322	[17]
120	21.68	Astragaloside IV [#]	$C_{41}H_{68}O_{14}$	$[M+COOH]-$	829.4580	829.4591	− 1.33	829.4580,783.4532,489.3586, 161.0449, 131.0234, 101.0234	[41]
121	21.71	Wogonoside	$C_{22}H_{20}O_{11}$	$[M+H]^+$	461.1062	461.1078	− 3.47	461.1062, 285.0753, 270.0518	[46]
122	21.90	Ginsenoside Ro [#]	$C_{48}H_{76}O_{19}$	$[M-H]^-$	955.4904	955.4908	− 0.42	955.4904, 793.4373, 731.4380, 569.3840, 523.3788	[37]
123	22.23	Apigenin	$C_{15}H_{10}O_5$	$[M+H]^+$	271.0597	271.0601	− 1.48	271.0597, 243.0645, 215.0701, 153.0181	[14, 46]
124	22.28	Licoricesaponin G2	$C_{42}H_{62}O_{17}$	$[M+H]^+$	839.4050	839.4060	− 1.19	839.4050, 469.3308	[14]
125	22.29	Neocnidilide	$C_{12}H_{18}O_2$	$[M+H]^+$	195.1378	195.1380	− 1.02	195.1378, 177.1271, 149.1324, 135.1167	[17]
126	22.35	9,12,13-trihydroxy − 10-octadecenoic acid [M]	$C_{18}H_{34}O_5$	$[M-H]^-$	329.2330	329.2333	− 0.91	329.2330, 229.1441, 211.1334	[39]
127	22.41	Baicalein or Norwogonin	$C_{15}H_{10}O_5$	$[M+H]^+$	271.0598	271.0601	− 1.11	271.0598, 243.0645, 215.0701, 153.0181	[46]
128	22.81	Calycosin isomer	$C_{16}H_{12}O_5$	$[M-H]^-$	283.0610	283.0612	− 0.71	283.0610, 268.0375, 224.0474, 211.0391, 135.0078	[41]
129	23.21	Astragaloside II [#]	$C_{43}H_{70}O_{15}$	$[M+COOH]-$	871.4697	871.4697	0.00	871.4697, 825.4590, 765.4442, 179.0560	[41]

Table 1 (continued)

Peak no	tR/min	Name	Formula	Mass ion type	Mean measured	Theoretical exact	Mass error(ppm)	Fragment ions	References
130	23.98	Pinocembrin [M]	$C_{15}H_{12}O_4$	$[M-H]^-$	255.0657	255.0663	− 2.35	255.0657, 135.0078, 119.0493	[41]
131	24.14	Gigantol	$C_{16}H_{18}O_4$	$[M+H]^+$	275.1275	275.1278	− 1.09	275.1275, 151.0752, 135.0596, 119.0493	[44]
132	24.36	Vestitol	$C_{16}H_{16}O_4$	$[M-H]^-$	271.0976	271.0976	0.00	271.0976, 256.0747, 149.0599, 135.0443	[18]
133	24.41	Formononetin [M]	$C_{16}H_{12}O_4$	$[M-H]^-$	267.0660	267.0663	− 1.12	267.0660, 252.0424, 223.0395, 195.0444	[18]
134	24.67	Z-6,7-epoxyligustilide	$C_{12}H_{14}O_3$	$[M+H]^+$	207.1012	207.1016	− 1.93	207.1012, 189.0908, 171.0802, 161.0958, 133.0283	[16]
135	24.74	Licoricesaponin E2	$C_{42}H_{60}O_{16}$	$[M-H]^-$	819.3803	819.3809	− 0.73	819.3803, 351.0562, 193.0347	—
136	24.85	Glyasperins M	$C_{21}H_{20}O_6$	$[M+H]^+$	369.1327	369.1333	− 1.63	369.1327, 313.0702, 285.0751, 271.0598	[14]
137	24.86	Uralsaponin B	$C_{42}H_{62}O_{16}$	$[M-H]^-$	821.3963	821.3965	− 0.24	821.3963, 351.0569, 193.0348	[41]
138	24.90	Soyasaponin I	$C_{48}H_{78}O_{18}$	$[M+H]^+$	943.5245	943.5261	− 1.70	943.5245, 599.3925, 441.3721, 423.3611	[41]
139	25.08	Isomucronulatol	$C_{17}H_{18}O_5$	$[M+H]^+$	303.1221	303.1227	− 1.98	303.1221, 193.0860, 181.0860, 167.0701, 123.0441	[46]
140	25.09	Senkyunolide D [M]	$C_{12}H_{14}O_4$	$[M-H]^-$	221.0814	221.0819	− 2.26	221.0814, 177.0913	[16]
141	25.44	Glyasperins B	$C_{21}H_{22}O_6$	$[M+H]^+$	371.1496	371.1489	1.89	371.1496, 353.1356, 315.0857, 297.0746, 175.0388, 147.0439	[18]
142	25.47	Glycyrrhizic acid [# M]	$C_{42}H_{62}O_{16}$	$[M-H]^-$	821.3961	821.3965	− 0.49	821.3961, 469.3346, 351.0563, 193.0347	[41]
143	25.57	Macranthoside A	$C_{47}H_{76}O_{17}$	$[M-H]^-$	911.5007	911.5010	− 0.33	911.5007, 821.4020, 702.8591	[47]
144	26.57	Senkyunolide C isomer	$C_{12}H_{12}O_3$	$[M+H]^+$	205.0858	205.0859	− 0.49	205.0858, 187.0752, 149.0233	[16]
145	26.71	Licorice saponine K2	$C_{42}H_{62}O_{16}$	$[M-H]^-$	821.3958	821.3965	− 0.85	821.3958, 351.0570, 193.0348	[41]
146	26.81	Glycycoumarin	$C_{21}H_{20}O_6$	$[M+H]^+$	369.1328	369.1333	− 1.35	369.1328, 313.0703, 285.0754	[14]
147	26.90	Isoastragaloside I	$C_{45}H_{72}O_{16}$	$[M+COOH]-$	913.4757	913.4802	− 4.93	913.4757, 867.4725, 513.1759	[41]
148	27.29	Glyasperins C	$C_{21}H_{24}O_5$	$[M-H]^-$	355.1559	355.1551	2.25	355.1559, 323.1285, 229.0866, 125.0234	[18]
149	27.45	Butylphthalide [M]	$C_{12}H_{14}O_2$	$[M+H]^+$	191.1064	191.1067	− 1.57	191.1064, 173.0959, 145.1011, 117.0700	[16]
150	27.47	Senkyunolide E	$C_{12}H_{12}O_3$	$[M-H]^-$	203.0707	203.0714	− 3.45	203.0707, 174.0314 130.0414	[16]
151	27.87	Chikusetsu saponin IVa	$C_{42}H_{66}O_{14}$	$[M-H]^-$	793.4370	793.4380	− 1.26	793.4370, 613.3704, 569.3859, 455.3530	[37]
152	28.20	Atractylenolide III [#]	$C_{15}H_{20}O_3$	$[M+H]^+$	249.1477	249.1485	− 3.21	249.1477,231.1378, 175.0754, 163.0752	[39]
153	28.61	Senkyunolide A	$C_{12}H_{16}O_2$	$[M+H]^+$	193.1222	193.1223	− 0.52	193.1222, 175.1116, 147.1168, 137.0596, 119.0856	[16]
154	28.63	Licoricone	$C_{22}H_{22}O_6$	$[M+H]^+$	383.1475	383.1489	− 3.65	383.1475, 327.0858, 299.0911	[18]
155	28.64	Isolicoflavonol	$C_{20}H_{18}O_6$	$[M-H]^-$	353.1027	353.1031	− 1.13	353.1027, 227.0709, 125.0235	[18]
156	29.19	Glycyrol	$C_{21}H_{18}O_6$	$[M-H]^-$	365.1027	365.1031	− 1.10	365.1027, 307.0247, 295.0245	[18]
157	29.47	*α*-Linolenic acid [M]	$C_{18}H_{30}O_2$	$[M+H]^+$	279.2314	279.2319	− 1.79	279.2314, 261.2206, 149.0232	[16]
158	30.81	E-ligustilide	$C_{12}H_{14}O_2$	$[M+H]^+$	191.1062	191.1067	− 2.62	191.1065, 173.0961, 145.1012	[16]
159	31.11	Glycyrin	$C_{22}H_{22}O_6$	$[M+H]^+$	383.1483	383.1489	− 1.57	383.1483, 327.0858, 299.0910	[18]
160	31.23	Z-ligustilide	$C_{12}H_{14}O_2$	$[M+H]^+$	191.1065	191.1067	− 1.05	191.1065, 173.0959, 145.1011, 117.0700	[16]
161	32.18	Atractylenolide II [# M]	$C_{15}H_{20}O_2$	$[M+H]^+$	233.1532	233.1536	− 1.72	233.1532, 215.1425, 187.1479, 151.0753, 105.0700	[39]
162	32.41	Glyasperins D	$C_{22}H_{26}O_5$	$[M+H]^+$	371.1836	371.1853	− 4.58	371.1836, 315.1221, 303.1221,235.1327, 167.0701, 123.0441	[18]
163	35.67	18-*β*-Glycyrrhetinic acid [M]	$C_{30}H_{46}O_4$	$[M+H]^+$	471.3465	471.3469	− 0.85	471.3465, 453.3361, 425.3408, 317.2114	[14]
164	36.43	Levistilide A	$C_{24}H_{28}O_4$	$[M+H]^+$	381.2056	381.2060	− 1.05	381.2056, 191.1065	[16]

[#] Confirmed with reference standards; [M]indicated components into the serum

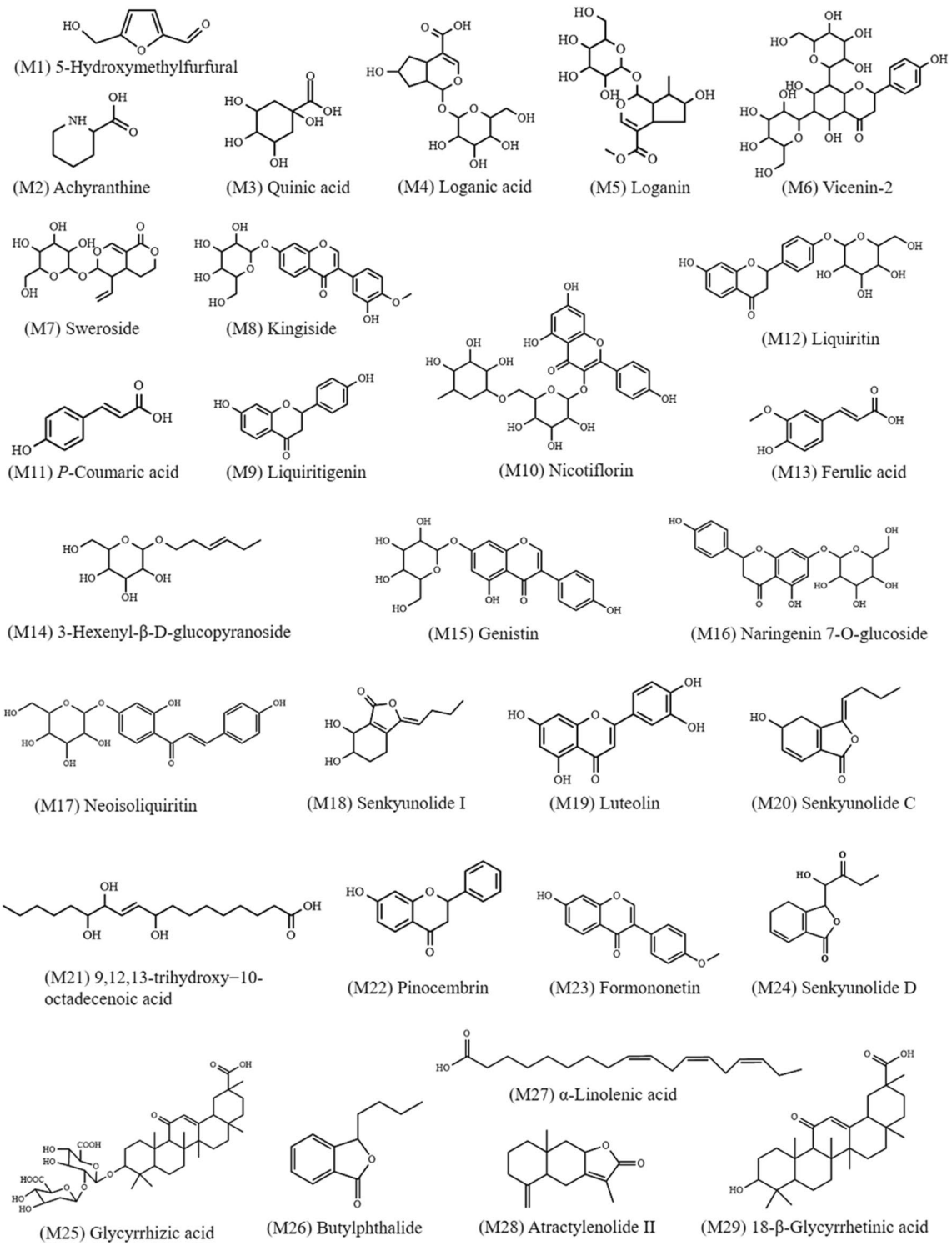

Fig. 3 Chemical structures of the 29 prototype compounds absorbed in TSMT-derived serum

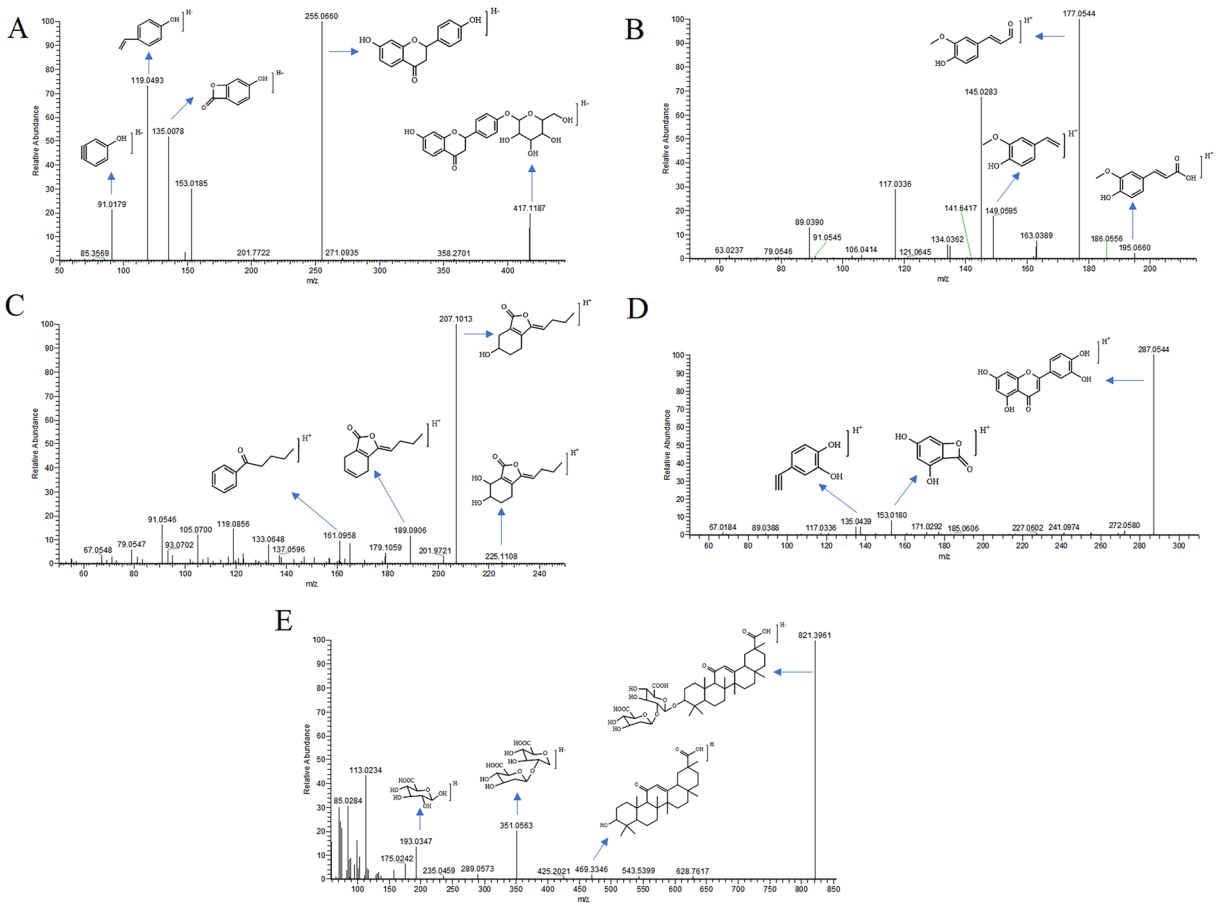

Fig. 4 Proposed mass fragments and fragmentation pathways of Liquiritin (**A**), Ferulic acid (**B**), Senkyunolide I (**C**), Luteolin (**D**), and Glycyrrhizic acid (**E**)

the correlation coefficients of similarity between nine batches of TSMT and simulated reference fingerprints.

Results

Identification of absorbable TSMT compounds

Both TSMT extracted sample and serum samples from mice administrated with TSMT were analyzed using UPLC-Q-Exactive Orbitrap/MS with positive and negative ion mode. The current total ion chromatograms of TSMT and serum sample were presented in Fig. 2. Based on the reference standards, and related studies comparing with the accurate mass and retention time information of compounds, we then characterized 164 chemical components from TSMT extraction in vitro. All detailed information was shown in Table 1.

A total of 29 constituents were generated from TSMT and absorbed into the serum. These were identified as prototype substances and their chemical structures were presented in Fig. 3. The selected crucial and representative fragmentation pathways of seven compounds absorbed into serum were analyzed in Fig. 4. For example, compound 68 (M12) was identified as Liquiritin at the retention time of 15.63 min, with the excimer ion peak of m/z 417.1187 $[M–H]^-$ ($C_{21}H_{22}O_9$) by compared with RS and related study [14]. The base peak was formed at m/z 255.0660 through the loss of a 162 Da glucose residue (–$C_6H_{10}O_5$) from the protonated ion. Also, another major fragment ion was produced at m/z 135.0078 ($C_7H_3O_3$) by simultaneous loss of 120 Da (–C_8H_8O) from m/z 255.0660. Further, the product ions were also obtained at m/z 119.0493 (–C_8H_7O) and m/z 91.0179. The cracking pattern of Liquiritin belonging to GC was shown in Fig. 4A. Similarly, compound 77 (M13) was characterized as Ferulic acid at the retention time of 16.39 min and the excimer ion peak at m/z 195.0660 $[M+H]^+$ ($C_{10}H_{10}O_4$) by compared with RS and many other studies [15]. The product ion was produced at m/z 177.0544 via elimination of a residue of one water molecule (18 Da). Another major fragment ion was produced at m/z 149.0595 by successive removal of one CO molecule (28 Da) from

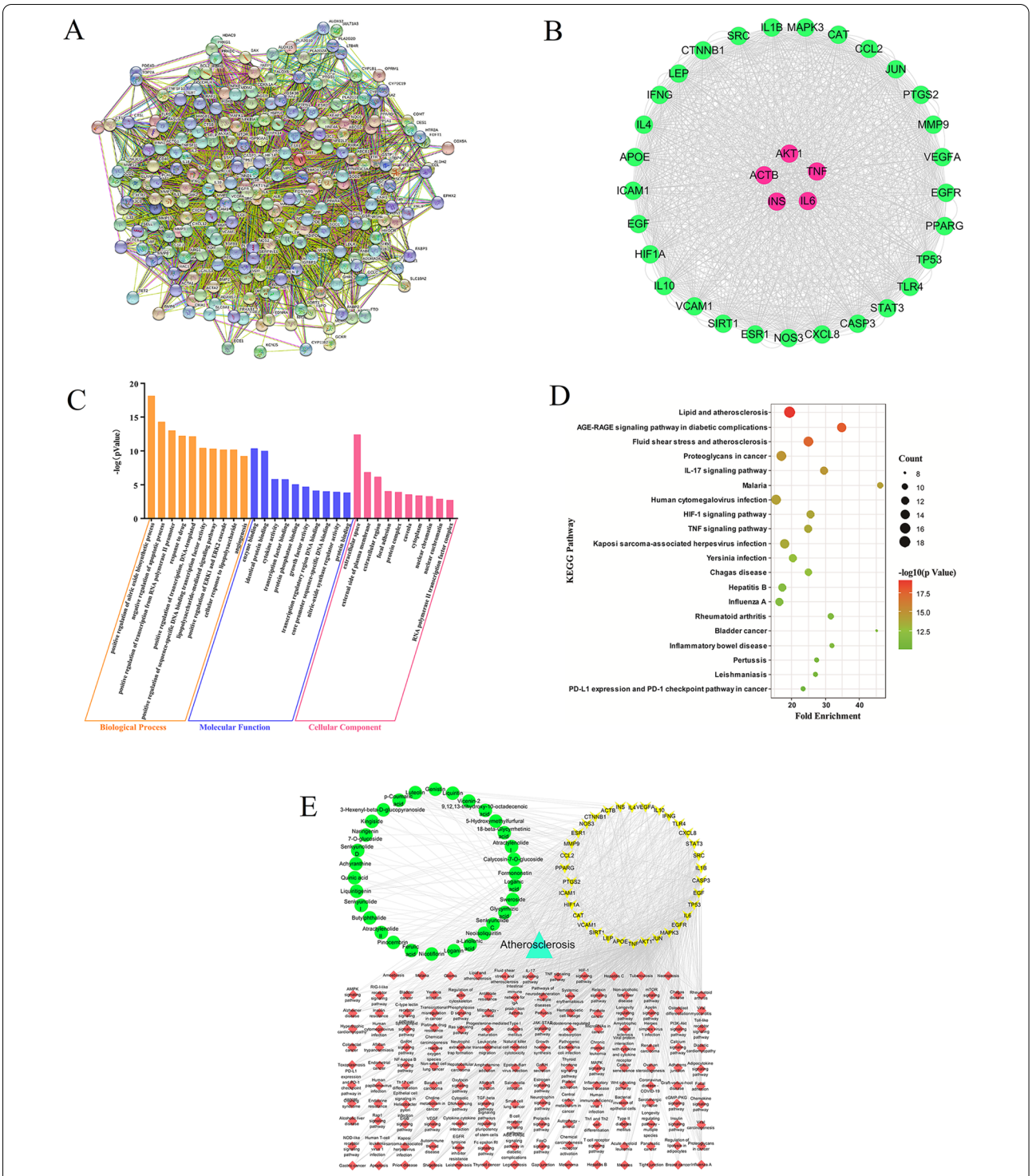

Fig. 5 Network pharmacology analysis of 29 serum-absorbed constituents of TSMT showing PPI network of 236 disease-drug targets (**A**), the module of selection of 34 hub targets (**B**), GO analysis (**C**), KEGG pathway enrichment (**D**) and the "Compounds-Targets -Pathways-Disease" network of TSMT in anti-AS mechanism (**E**) (This network consisted of 215 nodes and 1170 edges. the green elliptical nodes represented 29 active therapeutic ingredients, yellow V Triangle nodes represented 34 overlapped hub gene, red diamond nodes represented 151 signaling pathways and the bright green triangle node represented atherosclerosis disease)

m/z 177.0541. The detailed cleavage information of ferulic acid derived from DG was displayed in Fig. 4B. Compound 101 (M18) was unequivocally identified as Senkyunolide I with 18.54 min by comparison with an authentic standard and a previous study [16], which produced a dominant deprotonated ion $[M+H]^+$ at m/z 225.1119 ($C_{12}H_{16}O_4$). A product ion was also observed at m/z 207.1013 and m/z 189.0906 presumably resulting from the loss of one and two H_2O molecule, respectively. Furthermore, the base peak was formed at m/z 161.0958 by the loss of two water and one CO molecules from the protonated ion. The information on fragment ions information of Senkyunolide I originating from DG was characterized in Fig. 4C. Compound 114 (M19) exhibited an $[M+H]^+$ ion at m/z 287.0544 with the retention time of 20.40 min, which corresponded to a unique elemental composition of $C_{15}H_{10}O_6$. Comparing our data with the previous report, the compound was identified as Luteolin [17]. The product ion at m/z 153.0180 and m/z 135.0439 was respectively obtained by the loss of 134 Da ($-C_8H_6O_2$), and 152 Da ($-C_7H_4O_4$) chemical structures from the protonated molecular ion of m/z 287.0544, respectively. The above-mentioned product ion of Luteolin derived from JYH was displayed in Fig. 4D. Compound 142 (M25) was consistent with the main characteristics of Glycyrrhizic acid ($C_{42}H_{62}O_{16}$), as per the comparison with RS and the related literature [14, 18]. It displayed an $[M-H]^-$ ion at m/s 821.3961 with a retention time of 25.47 min. In the subsequent MS cleavage process, a chemical structure of 352 Da ($-C_{12}H_{16}O_{12}$) was removed from the quasi-molecular ion to form the characteristic fragment ion at m/z 469.3346, which corresponded to a molecular structure of Glycyrrhetinic acid. Simultaneously, the product ion was also detected at m/z 193.0347 through the loss of a chemical structure of 158 Da ($-C_6H_6O_5$) from the ion at m/z 351.0563. The proposed fragmentation of Glycyrrhizic acid derived from GC was given in Fig. 4E.

Network pharmacology analysis

Collection of key therapeutic targets and analysis of PPI construction

The absorbed compounds were used to predict the potential anti-AS targets and pathways of TSMT via our network pharmacology tool, whose results are shown in Table 1. The compounds or disease targets were searched in the databases and 236 intersection targets were screened out. These targets were imported into the STRING database and the relationship of Protein–Protein-Interaction (PPI) targets was documented in Fig. 5A, initially. This data was further imported into Cytoscape3.7.1 software for Network Analyze with three important topological parameters of Degree, Betweenness, and Closeness. Among them, Degree is considered of great importance as it was the center of the node and reflected connectedness of targets participating in the pathological process of diseases, implying that a larger degree value indicated more involvement in the disease process. Ultimately, 34 targets with higher protein interaction relationships (degree value greater than 99) we visualized and selected. Moreover, the top 3 targets namely the IL-6 (Degree = 182), TNF (Degree = 182), and AKT1 (Degree = 180), showed the greatest correlation with the active compounds useful in the treatment of AS. The detailed network topology of the 34 therapeutic targets was shown in Fig. 5B and Additional file 1: Table S1. Therefore, these 34 therapeutic targets were considered as the core targets of TSMT in the treatment of AS.

Enrichment analysis of GO gene function and KEGG pathway

To clarify the underlying anti-AS mechanism associated with TSMT therapeutic compounds, GO enrichment and KEGG pathway analyses were performed in combination with overlapped gene analysis. The GO gene analysis (detailed information given in Additional file 1: Table S2) suggested that 34 key target functions were related to biological process, molecular function and cellular components, such as enzyme binding, identical protein, etc. While, the KEGG enrichment analysis indicated that TSMT may be involved in 151 potential pathways (p value < 0.01), including the five predominant pathways involving lipid and atherosclerosis, fluid shear stress and atherosclerosis, IL-17 signaling pathway, HIF-1 signaling pathway, and TNF signaling pathway (detailed information given in Additional file 1: Table S3). Interestingly, R 4.0.3 software was used to visualize the top 10 GO categories and 20 KEGG pathways, which were presented in Fig. 5C and D, respectively. The enrichment analysis revealed that 29 compounds validated in the TSMT serum samples may play crucial roles in the treatment of AS by adjusting the above-mentioned diversified biological processes and signaling pathways.

Selection of the quality control (QC) markers

To explore the QC markers, a "components-key targets-functional pathways-disease" network was constructed using Cytoscape 3.7.1 software, which is represented in Fig. 5E. The Network Analyze was used to analyze the network relationship, which is displayed in Additional file 1: Table S4. With the degree value of greater than or equal to four, 18 potentially effective constituents were preliminarily screened out, which included Ferulic acid, Genistin, Glycyrrhizic acid, 18-β-Glycyrrhetinic acid, Luteolin, Formononetin, α-Linolenic acid, Liquiritigenin, ρ-Coumaric acid, Senkyunolide C, Pinocembrin, Liquiritin, Neoisoliquiritin, Atractylenolide II, Quinic acid,

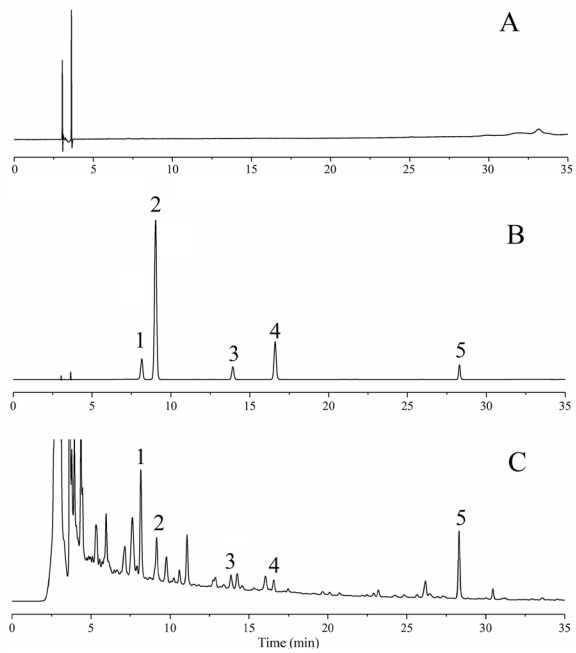

Fig. 6 HPLC chromatograms of negative control (**A**), mixed reference substance (**B**), and TSMT samples (**C**). Peak 1–5 represented Liquiritin, Ferulic acid, Senkyunolide I, Luteolin, and Glycyrrhizic acid, respectively

Loganin, 3-Hexenyl-beta-D-glucopyranoside, and Senkyunolide I. For example, Ferulic acid with 15 nodes showed the maximum degree of correlation followed by the Glycyrrhizic acid and Genistin showing the same relation degree at 12 nodes.

According to the "specificity", "efficacy correlation of TCM theory" and "measurability", of substances [19], Ferulic acid is tested as the quality standard marker for DG while Luteolin was the glycoside of cynaroside which is the quality marker of JYH. Liquiritin and Glycyrrhizic acid ate both derived from the quality standard marker of DC and are specified in the *Chinese Pharmacopoeia* (2020 edition). Additionally, DG is a sovereign drug imparting better benefits to the quality evaluation of TSMT. It consists of 5 potentially selected effective constituents, namely Senkyunolide I, Senkyunolide C, Senkyunolide D, Butylphthalide and α-Linolenic acid. Although, Senkyunolide I in TSMT could be measured by the current HPLC method, and Senkyunolide C, Senkyunolide D, Butylphthalide and α-Linolenic acid could not be detected possibly due to the polarity and low content of these chemical components in TSMT. Hence, to screen potential QC markers using network pharmacology, we selected 5 out of 29 common potentially effective anti-AS ingredients, including Liquiritin, Ferulic acid, Senkyunolide I, Luteolin, and Glycyrrhizic acid. Based on the degree of network, professional knowledge and literature validation, these five ingredients were considered potential quality markers of TSMT.

Simultaneous quantitative analysis of the five potentially effective ingredients

To select effective components through network pharmacological prediction, we considered multifaceted factors including the detection limit of the HPLC instrument, content levels in the TSMT components, and the measurability and availability of components. Next, we chose five active constituents including Liquiritin, Ferulic acid, Senkyunolide I, Luteolin, and Glycyrrhizic acid to establish the quality standards of multiple batches of TSMT by simultaneously determining their contents. Meanwhile, the obtained chromatographic peaks of these five components showed good resolution and detection performance due to the optimized HPLC conditions. Since the calibration curves of all reference substances were linear in the determinable range ($r > 0.9997$), the validation of the method was verified. Additionally, this measurable method also showed satisfactory precision, repeatability, and stability of all relative analytes because the relative

Table 2 Content determination of the five markers in nine batches of TSMT

No.	Liquiritin (mg/g)	Ferulic acid (mg/g)	Senkyunolide I (mg/g)	Luteolin (mg/g)	Glycyrrhizic acid (mg/g)
S1	1.8195	0.6594	0.7801	0.1910	5.7449
S2	1.8148	0.6722	0.7738	0.1921	5.7317
S3	1.8102	0.6916	0.7797	0.1928	5.7632
S4	1.8195	0.6796	0.7444	0.1882	5.7428
S5	1.8338	0.6746	0.7782	0.1939	5.7763
S6	1.8500	0.6868	0.8054	0.1983	5.8477
S7	1.8720	0.6618	0.7634	0.1979	5.9022
S8	1.8341	0.6718	0.7807	0.1920	5.7520
S9	1.8006	0.6660	0.7621	0.1895	5.6651

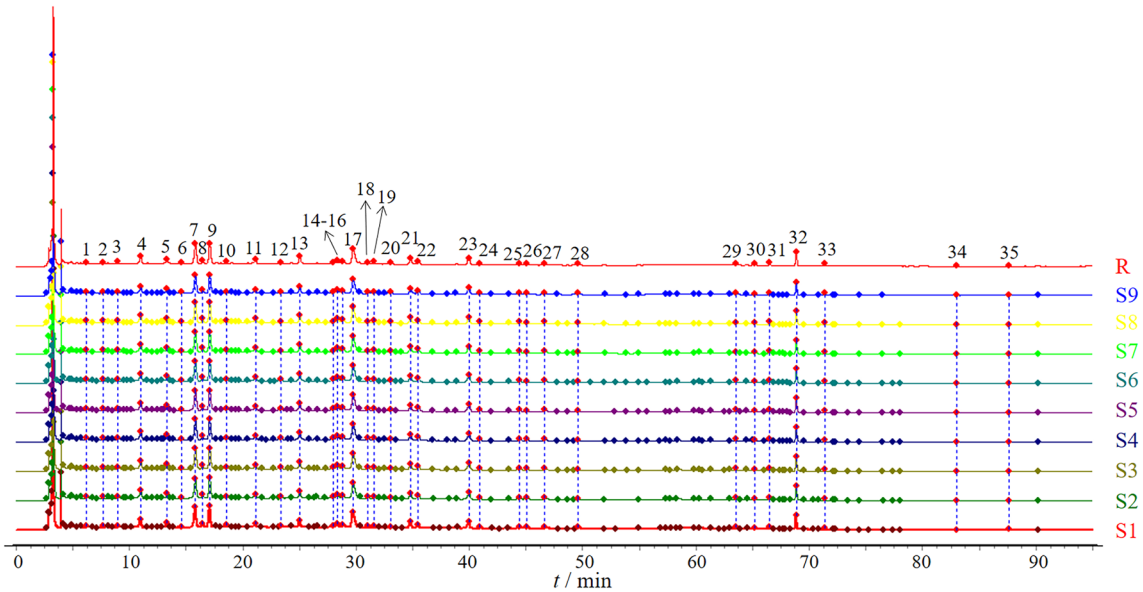

Fig. 7 HPLC fingerprints of the reference (R) and S1–S9 in TSMT samples (R indicates fingerprints of reference; S1–S9 represents nine batches of TSMT sample in sequence)

standard deviation (RSD%) of the peak area was less than 3% while the average recoveries ranged from 98.9% to 99.7%. This indicated that the quantitative determination method was feasible and reliable for simultaneous determination of the five potential active ingredient markers, which was demonstrated in Additional file 1: Table S5. The HPLC chromatogram of samples was displayed in Fig. 6.

Simultaneously, the above-described method was also applied to quantify five ingredients of TSMT. The average contents of the five components in nine batches of TSMT were showed in Table 2. The results showed that TSMT constituted Liquiritin (1.8006 ~ 1.8720 mg/g), Ferulic acid (0.6594 ~ 0.6916 mg/g), Senkyunolide I (0.7444 ~ 0.8054 mg/g), Luteolin (0.1882 ~ 0.1979 mg/g) and Glycyrrhizic acid (5.6651 ~ 5.9022 mg/g) in high quantities. Generally, 70% of the mean value is considered as the standard limit for the component content of Chinese patent medicines. Thereby, TSMT may contain Liquiritin, Ferulic acid, Senkyunolide I, Luteolin, and Glycyrrhizic acid in quantity not less than 1.2798, 0.4716, 0.5419, 0.1349, 4.0386 mg/g, respectively, indicating that these five compounds may serve as the major bioactive markers of TMST.

Establishment of chemical fingerprints in nine batches of TSMT

The optimized chromatographic conditions resulted in the good separation of the constituents in all samples. Also, the results of methodology validation were satisfactory with high precision, good repeatability and high stability. Since the RSD% values of precision, repeatability, and stability in the S1 sample were less than 3%, it was beneficial for the fingerprint analysis of TSMT. Fingerprint analysis was established based on HPLC data of nine batches of TSMT (S1–S9). All the data were entered into the Similarity Evaluation System for Chromatographic Fingerprint of Traditional Chinese Medicines (2012 version) to obtain common peaks with a peak area of more than 0.09% of the total peak area during the match. A total of 35 common peaks (peak 1–35) were found in these chromatograms along with a reference fingerprint (R) spectrum (Fig. 7).

The similarity values of HPLC fingerprints were matched by calculating correlative coefficients between the TSMT samples and reference fingerprint (R). The similarities were evaluated at a value greater than 0.998 (detailed similarity analysis displayed in Additional file 1: Table S6). Based on the known reference substances and their medicinal origin, common peaks of 14, 17, 23, 28, and 32 were identified as Ferulic acid (belonging to DG), Liquiritin (belonging to GC), Senkyunolide I (belonging to DG), Luteolin (belonging to JYH), and Glycyrrhizic acid (belonging to GC), respectively. Therefore, a fingerprint analysis with a good profile of chromatographic peaks indicated a stable prescription process while the main chemical constituents of the different batches of TSMT prescription showed no significant influence overall.

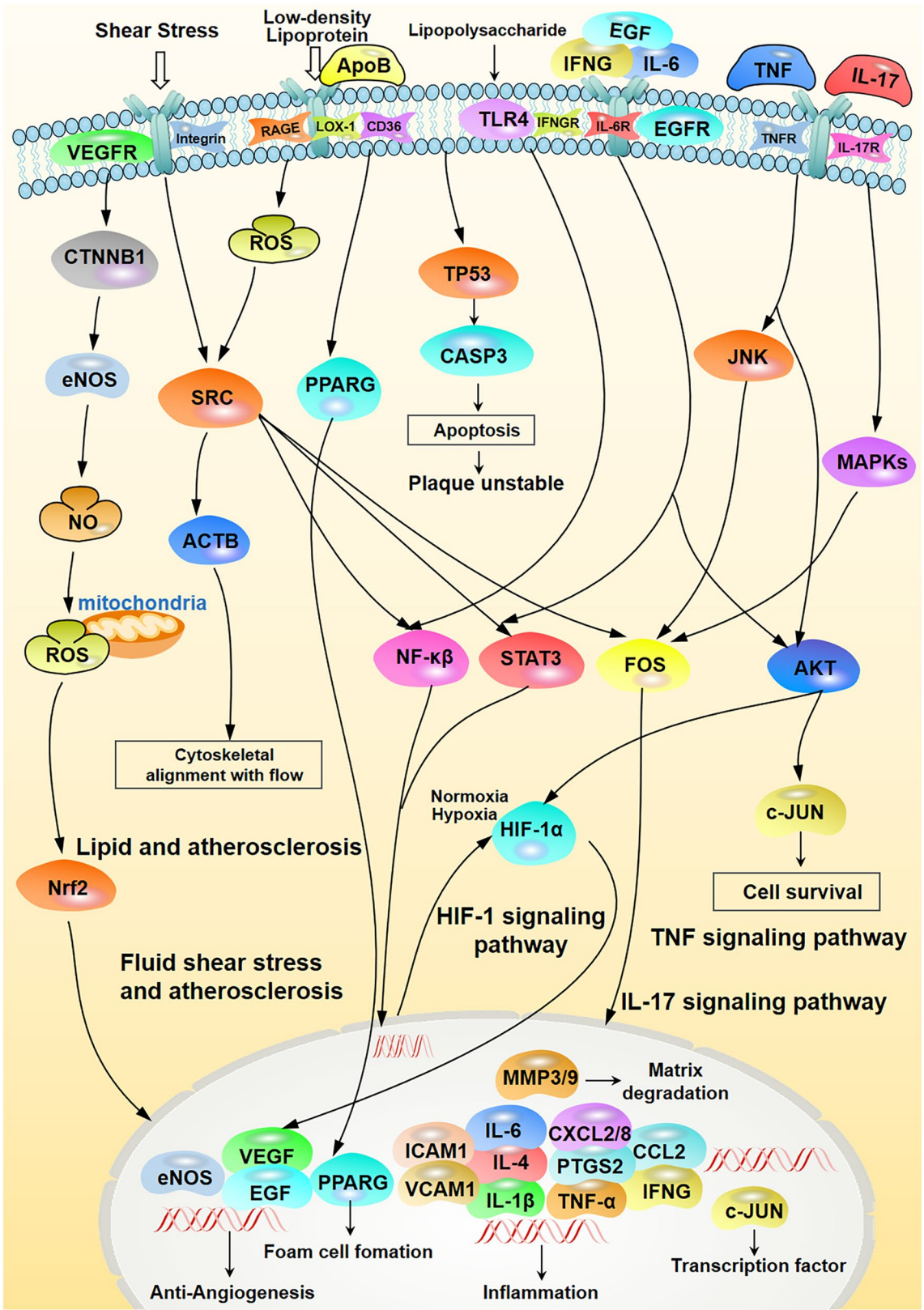

Fig. 8 Predicted and related anti-AS mechanisms of TSMT

Discussion

According to the TCM theory, Tongsaimai tablet (TSMT), a commercial Chinese patent medicine, exhibited a definite medicinal effect of promoting blood circulation, dredging collaterals, tonifying qi, and nourishing Yin. The current quality standards of TSMT by CFDA (YBZ08372004) suggest chlorogenic acid, derived from JYH, as the content determination index [10]. However, the quantitative determination of only chlorogenic acid cannot fully reflect the TSMT quality. Also, the QC markers of most TCM prescriptions are selected based on the specificity of compounds mentioned in Chinese Pharmacopoeia (2020 edition). The quality standard for DG was established by determining the content of Ferulic acid in TSMT using HPLC. The quality control index compound of JYH is Cynaroside which produces an aglycon of Luteolin. Similarly, Harpagoside and Harpagoside, Astragaloside IV and Calycosin-7-glucoside, β-Ecdysterone, Dendrobium and Erianin, and Liquiritin and Glycyrrhizic acid can be used as marker compounds for XS, HQ, NX, SH and GC, respectively.

Atherosclerosis (AS) is a chronic vascular disease whose pathogenic mechanism begins with endothelial cell (EC) damage occurring due to lipid accumulation in blood vessels, followed by abnormal lipid metabolism of cholesterol including low-density lipoprotein (LDL) and recruitment of macrophages to the arterial walls [20]. The deposition of subendothelial lipoproteins leads to the aggregation of monocytes, that later differentiate into macrophages in the intimal compartment [21]. Macrophages uptakes oxidation-modified lipoproteins such as oxidized low-density lipoproteins (ox-LDLs) excessively and disorderly which mediated by scavenger receptors to form cholesterol-overloaded foam cells [22]. Furthermore, these foam cells trigger a series of inflammatory reactions, contributing to the necrotic core formation of atheromatous plaques. In this study, we identified 29 key active ingredients related with 34 core genes and 151 signaling pathways. Next, we constructed the pharmacological network of the anti-AS mechanism of TSMT. Consequently, we found that the function of AS was improved by five central pathways, including lipid and atherosclerosis, fluid shear stress and atherosclerosis, IL-17 signaling pathway, HIF-1 signaling pathway, and TNF signaling pathway, which were found closely related to the different regulations of anti-angiogenesis, foam cell formation, cytoskeletal alignment with the flow, inflammation, matrix degradation, and plaque instability by apoptosis (Fig. 8). Our analysis further clarified the potential mechanisms of TSMT against AS and demonstrated that the chief association of these anti-AS pathways were chiefly associated with the main response of lipid regulation, fluid shear stress, and inflammation. Lipid and atherosclerosis pathway is found significantly associated with lipid metabolism. Consistent with various studies [7–9], our results indicated that TSMT may improve the lipid disorder effect by inhibiting lipid plaque through close association with anti-inflammatory activities and antioxidative stress. Shear stress (also called frictional force), a local hemodynamic factor, is generated on the endothelial cell surface by blood flow. Low shear stress (LSS) is prevalent at the AS-prone sites [23]. Some studies have emphasized that focus on the early stages of AS, where anti-inflammatory and anti-oxidative activities could together regulate LSS [24, 25]. Moreover, IL-17 signaling pathways and TNF signaling pathways also play an indispensable role in inflammatory effects. In a previous study, the activation of IL-17 signaling pathways and TNF signaling pathways regulated pro-inflammatory and pro-atherogenic cytokines such as IL-1β, IL-6, TNF, along with activating transcription factors such as FOS and JUN [26]. Hypoxia has been demonstrated in AS progression while HIF-1 has been found to promote intraplaque angiogenesis and the development of foam cells. HIF-1α modulation can stimulate multiple factors related to the secretion of Akt, VEGF, and CXCL-8, which blocks atherosclerotic plaque development and reduces intrinsic inflammatory responses [27]. Increasing evidences have demonstrated a probable association of HIF-1 signaling pathway with the formation of foam cell, inflammatory action of macrophages, and angiogenesis preventing the development of AS [28, 29]. Therefore, through the above-mentioned mechanisms, TSMT could prevent AS by regulating lipid metabolism, inflammatory response and oxidative stress, hemodynamic shear stress, anti-angiogenic effects, etc.

In our study, we initially selected five effective prototype constituents such as Ferulic acid, Liquiritin, Senkyunolide I, Luteolin, and Glycyrrhizic acid as indicators, which were obtained from the component-target network through qualitative and quantitative HPLC analysis. Modern pharmacological studies have reported that these five compounds exerted anti-AS effects. Ferulic acid has exhibited anti-atherogenic properties by significantly regulating lipid metabolism in high-fat diet-induced ApoE−/− mouse model. It also effectively improves the expression of mitochondrial function while reducing the oxidative stress during vascular damage of endothelial cells and human mononuclear cells in the mouse model of AS [30, 31]. Senkyunolide I may alleviate thrombosis as a key pathological event in cardiovascular disease, affecting the inhibition of platelet activation, coagulation cascade, oxidative stress, endoplasmic reticulum stress, and apoptosis [32, 33]. Luteolin inhibits the adhesion of TNF-α induced monocytes to endothelial cells by blocking CCL2, ICAM-1, and VCAM-1 expression along with

suppressing the IκBα/NF-κB mediated signaling pathway [34]. Liquiritin performs anti-inflammatory activities in LPS-stimulated mouse brain microglia cell by inhibiting pro-inflammatory mediators such as iNOS, PTGS2, TNF-α, IL-1β, and IL-6 [35]. Glycyrrhizic acid has exerted an atheroprotective effect in AS treatment by improving lipid metabolism. It decreases the serum lipid levels and atherosclerotic plaque deposition, and further suppresses vascular inflammation in Th17 cells in ApoE−/− mice by reducing IL-6 and STAT3 phosphorylation [36].

Conclusion

In this study, serum pharmacochemistry and network pharmacology were integrated to establish the quality assessment of TSMT along with exploring the related underlying mechanisms of TSMT in AS alleviation. The component-target-pathway network was used to screen five potentially bioactive ingredients in TSMT, which included Ferulic acid, Liquiritin, Senkyunolide I, Luteolin and Glycyrrhizic acid. These sere considered as the potential QC markers. Based on these selected indexes, HPLC–DAD analysis and HPLC fingerprint method were performed for simultaneous multi-component determination, which helped in assessing the quality of nine batches of TSMT samples. In summary, this study may provide substantial evidence to improve the quality control of TSMT, greatly facilitating the efficacy and safety of TSMT in clinical applications. To the best of our knowledge, this is the first attempt to explore the potential anti-AS mechanism and establish a quality control system to provide comprehensive quality of TSMT.

Abbreviations

TSMT: Tongsaimai tablet; CFDA: China Food and Drug Administration; TCM: Traditional Chinese Medicine; AS: Atherosclerosis; QC: Quality control; HPLC: High performance liquid chromatography; DAD: Diode array detector; RSD: Relative standard deviation.

Supplementary Information

The online version contains supplementary material available at https://doi.org/10.1186/s13020-022-00658-9.

Additional file 1: Table S1. Network topological analysis of 34 core therapeutic targets in PPI network. **Table S2**. TSMT improves TOP 10 GO categories of core targets of atherosclerosis. **Table S3**. TSMT alleviates TOP 20 KEGG pathway of core targets of atherosclerosis. **Table S4**. Crucial anti-AS ingredients were selected as candidate active compounds in TSMT. **Table S5**. Methodological investigation results of the content determination method of TSMT. **Table S6**. Similarity evaluation results of HPLC fingerprint of nine batches of S1-S9 in TSMT.

Acknowledgements

Not applicable.

Author contributions

YC: Investigation, Writing-original draft preparation, Writing-review and editing. MX: Methodology, Writing—original draft, and Writing—review & editing. JC: Software, Visualization. DW: Validation, Investigation. CZ: Methodology, Validation. TW: Methodology, Validation. YH: Conceptualization, Writing-original draft preparation, Writing-review and editing, Supervision. CF: Conceptualization, Resources, Funding acquisition, Supervision. YW: Investigation, Writing-original draft preparation, Writing-review and editing, Supervision. JZ: Conceptualization, Resources, Funding acquisition, Supervision. All data were generated in-house, and no paper mill was used. All authors agree to be accountable for all aspects of work ensuring integrity and accuracy. All authors read and approved the final manuscript.

Funding

This work was supported by Open Fund project of State Key Laboratory of New-tech for Chinese Medicine Pharmaceutical Process (SKL2020Z0303) and Sichuan Science and Technology Innovation Miao Zi Project (2021083).

Availability of data and materials

The datasets used and/or analyzed during the current study are available from the corresponding author on reasonable request.

Declarations

Ethics approval and consent to participate

The animal experiments were approved by the ethics committee of the Chengdu University of Traditional Chinese Medicine (CDUTCM, permit CDU2020KB097), and were conducted in strict accordance with the Guidelines for the Use Committee 520 (IACUC) of Chengdu University of Traditional Chinese Medicine.

Consent for publication

Not applicable.

Competing interests

The authors declare that they have no competing interests.

Author details

[1]State Key Laboratory of Southwestern Chinese Medicine Resources, School of Pharmacy, Chengdu University of Traditional Chinese Medicine, Chengdu 611137, China. [2]Key Laboratory of Coarse Cereal Processing, Ministry of Agriculture and Rural Affairs, Chengdu University, Chengdu 610106, Sichuan, China. [3]Jiangsu Kanion Pharmaceutical CO. LTD, Lianyungang 222001, China. [4]State Key Laboratory of New-Tech for Chinese Medicine Pharmaceutical Process, Lianyungang 222001, China.

Received: 12 May 2022 Accepted: 22 August 2022
Published online: 02 September 2022

References

1. Khyzha N, Alizada A, Wilson MD, Fish JE. Epigenetics of atherosclerosis: emerging mechanisms and methods. Trends Mol Med. 2017;23(4):332–47.
2. Song P, Fang Z, Wang H, Cai Y, Rahimi K, Zhu Y, Fowkes FGR, Fowkes FJI, Rudan I. Global and regional prevalence, burden, and risk factors for carotid atherosclerosis: a systematic review, meta-analysis, and modelling study. Lancet Glob Health. 2020;8(5):e721–9.
3. Adhyaru BB, Jacobson TA. Safety and efficacy of statin therapy. Nat Rev Cardiol. 2018;15(12):757–69.
4. Yang X, Sun L, Li Y, Ma C, Yang J, Zhang W, Zhao B, Jia L, Duan Y, Han J, et al. NaoXinTong inhibits the advanced atherosclerosis and enhances the plaque stability in apolipoprotein E deficient mice. J Cardiovasc Pharmacol. 2016;67(3):203–11.
5. Wang C, Niimi M, Watanabe T, Wang Y, Liang J, Fan J. Treatment of atherosclerosis by traditional Chinese medicine: questions and quandaries. Atherosclerosis. 2018;277:136–44.

6. Zhao Y, Zhang QC, Zhu Q, Yin SM, Wen HM, Bian HM. Effects and mechanism of five Chinese patent medicines on focal cerebral ischemia. Zhong yao cai = Zhongyaocai = J Chin Med Mater. 2011;34(6):927–31.
7. Yang Y, HU C, Bian H, Dai X. Effect of Tongsaimai Tablet on experimental atherosclerosis in rats. Chin Tradit Pat Med. 2010; 32(03):371–374.
8. Qiu J, Bian H, Zhang Q, Gao C. Effect of Tongsaimai tablets on rats' experimental hyperlipidemia and atherosclerosis. Shanghai J Tradit Chin Med. 2007;41(01):71–3.
9. Xiu Y, Hu C, Jiang F, Yin S, Bian H. Effect of Tongsaimai Tablet on MMP-9/TIMP-1 in atherosclerotic rats. J Nanjing TCM Univ. 2010;26(03):208–10.
10. Zhang S, Gong L, Guo Q. Study on quality standard of Tongsaimai Tablets. J Tradit Chin Med. 2013;35(07):1568–73.
11. Wu Y, Cheng Y, Yang Y, Wang D, Yang X, Fu C, Zhang J, Hu Y. Mechanisms of Gegen Qinlian Pill to ameliorate irinotecan-induced diarrhea investigated by the combination of serum pharmacochemistry and network pharmacology. J Ethnopharmacol. 2021;276: 114200.
12. Wang X. Studies on serum pharmacochemistry of traditional Chinese medicine. World Sci Technol/Mod Trad Chin Med. 2002;4(02):1–4+78.
13. Wang L, Pu X, Nie X, Wang D, Jiang H, Chen Y, Pang L, Wang S, Wang X, Xu Z, et al. Integrated serum pharmacochemistry and network pharmacological analysis used to explore possible anti-rheumatoid arthritis mechanisms of the Shentong-Zhuyu decoction. J Ethnopharmacol. 2021;273: 113988.
14. Hu Y, Xu W, Qin X, Liu Y. Rapid identification of chemical constituents in Huangqi Jianzhong Tang by UHPLC coupled with hybrid quadrupole-orbitrap MS. Acta Pharm Sin. 2017;52(06):964–70.
15. Wang S, Xu X, Liu X. Analysis of differential chemical constituents in scrophulariae radix from different areas using UFLC-triple TOF-MS /MS. Chin Pharm J. 2019;54(09):741–8.
16. Wang L, Huang S, Chen B, Zang XY, Su D, Liang J, Xu F, Liu GX, Shang MY, Cai SQ. Characterization of the anticoagulative constituents of angelicae sinensis radix and their metabolites in rats by HPLC-DAD-ESI-IT-TOF-MSn. Planta Med. 2016;82(4):362–70.
17. Liang J, Gao H, Chen L, Xiao W, Wang Z, Wang Y, Wang Z. Chemical profiling of an antimigraine herbal preparation, Tianshu capsule, based on the combination of HPLC, LC-DAD-MS (n), and LC-DAD-ESI-IT-TOF/MS analyses. Evid Based Complement Alternat Med. 2014;2014: 580745.
18. Wang X, Liu X, Xu X, Zhu T, Shi F, Qin K, Cai B. Screening and identification of multiple constituents and their metabolites of Fangji Huangqi Tang in rats by ultra-high performance liquid chromatography coupled with quadrupole time-of-flight tandem mass spectrometry basing on coupling data processing techniques. J Chromatogr B Analyt Technol Biomed Life Sci. 2015;985:14–28.
19. Zhang TJ, Bai G, Chen CQ, Xu J, Han YQ, Gong SX, Zhang HB, Liu CX. Research approaches of quality marker (Q-marker) of Chinese materia medica formula based on "five principles." Zhong Cao Yao. 2018;49(01):1–13.
20. Moore KJ, Tabas I. Macrophages in the pathogenesis of atherosclerosis. Cell. 2011;145(3):341–55.
21. Gimbrone MA Jr, García-Cardeña G. Endothelial cell dysfunction and the pathobiology of atherosclerosis. Circ Res. 2016;118(4):620–36.
22. Checkouri E, Ramin-Mangata S, Diotel N, Viranaicken W, Marodon C, Reignier F, Robert-Da Silva C, Meilhac O. Protective effects of medicinal plant decoctions on macrophages in the context of atherosclerosis. Nutrients. 2021;13(1):280.
23. Souilhol C, Serbanovic-Canic J, Fragiadaki M, Chico TJ, Ridger V, Roddie H, Evans PC. Endothelial responses to shear stress in atherosclerosis: a novel role for developmental genes. Nat Rev Cardiol. 2020;17(1):52–63.
24. Siasos G, Sara JD, Zaromytidou M, Park KH, Coskun AU, Lerman LO, Oikonomou E, Maynard CC, Fotiadis D, Stefanou K, et al. Local low shear stress and endothelial dysfunction in patients with nonobstructive coronary atherosclerosis. J Am Coll Cardiol. 2018;71(19):2092–102.
25. Malek AM, Alper SL, Izumo S. Hemodynamic shear stress and its role in atherosclerosis. JAMA. 1999;282(21):2035–42.
26. Li G, Xu Q, Han K, Yan W, Huang C. Experimental evidence and network pharmacology-based analysis reveal the molecular mechanism of Tongxinluo capsule administered in coronary heart diseases. 2020. Biosci Rep. https://doi.org/10.1042/BSR20201349.
27. Gessi S, Fogli E, Sacchetto V, Merighi S, Varani K, Preti D, Leung E, Maclennan S, Borea PA. Adenosine modulates HIF-1{alpha}, VEGF, IL-8, and foam cell formation in a human model of hypoxic foam cells. Arterioscler Thromb Vasc Biol. 2010;30(1):90–7.
28. Liu D, Lei L, Desir M, Huang Y, Cleman J, Jiang W, Fernandez-Hernando C, Di Lorenzo A, Sessa WC, Giordano FJ. Smooth muscle hypoxia-inducible factor 1alpha links intravascular pressure and atherosclerosis-brief report. Arterioscler Thromb Vasc Biol. 2016;36(3):442–5.
29. Aarup A, Pedersen TX, Junker N, Christoffersen C, Bartels ED, Madsen M, Nielsen CH, Nielsen LB. Hypoxia-inducible factor-1alpha expression in macrophages promotes development of atherosclerosis. Arterioscler Thromb Vasc Biol. 2016;36(9):1782–90.
30. Gu Y, Zhang Y, Li M, Huang Z, Jiang J, Chen Y, Chen J, Jia Y, Zhang L, Zhou F. Ferulic acid ameliorates atherosclerotic injury by modulating gut microbiota and lipid metabolism. Front Pharmacol. 2021;12: 621339.
31. Perez-Ternero C, Werner CM, Nickel AG, Herrera MD, Motilva MJ, Bohm M, Alvarez de Sotomayor M, Laufs U. Ferulic acid, a bioactive component of rice bran, improves oxidative stress and mitochondrial biogenesis and dynamics in mice and in human mononuclear cells. J Nutr Biochem. 2017;48:51–61.
32. Li J, Liu H, Yang Z, Yu Q, Zhao L, Wang Y. Synergistic effects of cryptotanshinone and Senkyunolide I in Guanxinning Tablet against endogenous thrombus formation in zebrafish. Front Pharmacol. 2020;11: 622787.
33. Zhu YL, Huang J, Chen XY, Xie J, Yang Q, Wang JF, Deng XM. Senkyunolide I alleviates renal ischemia-reperfusion injury by inhibiting oxidative stress, endoplasmic reticulum stress and apoptosis. Int Immunopharmacol. 2022;102: 108393.
34. Jia Z, Nallasamy P, Liu D, Shah H, Li JZ, Chitrakar R, Si H, McCormick J, Zhu H, Zhen W, et al. Luteolin protects against vascular inflammation in mice and TNF-alpha-induced monocyte adhesion to endothelial cells via suppressing IKappaBalpha/NF-kappaB signaling pathway. J Nutr Biochem. 2015;26(3):293–302.
35. Yu JY, Ha JY, Kim KM, Jung YS, Jung JC, Oh S. Anti-inflammatory activities of licorice extract and its active compounds, glycyrrhizic acid, liquiritin and liquiritigenin, in BV2 cells and mice liver. Molecules. 2015;20(7):13041–54.
36. Yang PS, Kim DH, Lee YJ, Lee SE, Kang WJ, Chang HJ, Shin JS. Glycyrrhizin, inhibitor of high mobility group box-1, attenuates monocrotaline-induced pulmonary hypertension and vascular remodeling in rats. Respir Res. 2014;15:148.
37. Jaiswal Y, Liang Z, Ho A, Chen H, Williams L, Zhao Z. Tissue-based metabolite profiling and qualitative comparison of two species of Achyranthes roots by use of UHPLC-QTOF MS and laser micro-dissection. J Pharm Anal. 2018;8(1):10–9.
38. Zhang YD, Huang X, Zhao FL, Tang YL, Yin L. Study on the chemical markers of Caulis Lonicerae japonicae for quality control by HPLC-QTOF/MS/MS and chromatographic fingerprints combined with chemometrics methods. Anal Methods. 2015;7(5):2064–76.
39. Gao S, Liu J, Wang M, Liu Y, Meng X, Zhang T, Qi Y, Zhang B, Liu H, Sun X, et al. Exploring on the bioactive markers of Codonopsis Radix by correlation analysis between chemical constituents and pharmacological effects. J Ethnopharmacol. 2019;236:31–41.
40. Ma XQ, Leung AK, Chan CL, Su T, Li WD, Li SM, Fong DW, Yu ZL. UHPLC UHD Q-TOF MS/MS analysis of the impact of sulfur fumigation on the chemical profile of Codonopsis Radix (Dangshen). Analyst. 2014;139(2):505–16.
41. Li Y, Liu J, Su R, Li Q, Chen Y, Yang J, Zhao S, Jia Z, Xiao H. Pseudotargeted screening and determination of constituents in Qishen granule based on compound biosynthetic correlation using UHPLC coupled with high-resolution MS. J Sep Sci. 2020;43(6):1032–42.
42. Xie G, Jiang Y, Huang M, Zhu Y, Wu G, Qin M. Dynamic analysis of secondary metabolites in various parts of Scrophularia ningpoensis by liquid chromatography tandem mass spectrometry. J Pharm Biomed Anal. 2020;186: 113307.
43. Kang J, Zhou L, Li Z, Sun Z, Wang X, Wang W, Zuo L, Zhang J, Liu L, Shi Y, et al. Chemical constituents study of compound Xueshuantong capsules based on UHPLC-Q-Orbitrap HRMS. Chin J Pharm Anal. 2019;39(05):791–804.
44. Yang J, Han X, Wang HY, Yang J, Kuang Y, Ji KY, Yang Y, Pang K, Yang SX, Qin JC, et al. Comparison of metabolomics of Dendrobium officinale in different habitats by UPLC-Q-TOF-MS. Biochem Syst Ecol. 2020. https://doi.org/10.1016/j.bse.2020.104007.

45. Ye Z, Dai JR, Zhang CG, Lu Y, Wu LL, Gong AGW, Xu H, Tsim KWK, Wang ZT. Chemical differentiation of Dendrobium officinale and Dendrobium devonianum by using HPLC fingerprints, HPLC-ESI-MS, and HPTLC analyses. Evid Based Complement Alternat Med. 2017;2017:8647212.
46. Xu R, Fan J, Dong H, Chen X, Xu J, Huo J, Ju J. UPLC-Q-TOF-MS analysis on chemical constituents of classical prescription Huangqi Guizhi Wuwu Tang standard decoction. China J Chin Mater Med. 2020;45(23):5614–30.
47. Liu H, Zheng YF, Li CY, Zheng YY, Wang DQ, Wu Z, Huang L, Wang YG, Li PB, Peng W, et al. Discovery of anti-inflammatory ingredients in Chinese herbal formula Kouyanqing granule based on relevance analysis between chemical characters and biological effects. Sci Rep. 2015;5:18080.
48. Wu Q, Yuan Q, Liu EH, Qi LW, Bi ZM, Li P. Fragmentation study of iridoid glycosides and phenylpropanoid glycosides in Radix Scrophulariae by rapid resolution liquid chromatography with diode-array detection and electrospray ionization time-of-flight mass spectrometry. Biomed Chromatogr. 2010;24(8):808–19.
49. Liang ZY, Zhang JY, Huang YC, Zhou CJ, Wang YW, Zhou CH, Xing SP, Shun QS, Xu YX, Wei G. Identification of flavonoids in Dendrobium huoshanense and comparison with those in allied species of Dendrobium by TLC, HPLC and HPLC coupled with electrospray ionization multi-stage tandem MS analyses. J Sep Sci. 2019;42(5):1088–104.
50. Zhang J, Xu W, Wang P, Huang J, Bai JQ, Huang ZH, Liu XS, Qiu XH. Chemical analysis and multi-component determination in Chinese Medicine preparation Bupi Yishen formula using ultra-high performance liquid chromatography with linear ion trap-orbitrap mass spectrometry and triple-quadrupole tandem mass spectrometry. Front Pharmacol. 2018;9:568.
51. An T, Chen X, Zhang M, Zhang Y. Rapid analysis on chemical constituents in roots of Codonopsis tangshen by UPLCcoupled with Q-exactive quadrupole-orbitrap mass spectrometry. Zhong Cao Yao. 2018;49(07):1533–42.
52. Chau SL, Huang ZB, Song YG, Yue RQ, Ho A, Lin CZ, Huang WH, Han QB. Comprehensive quantitative analysis of SQ injection using multiple chromatographic technologies. Molecules. 2016. https://doi.org/10.3390/molecules21081092.

Publisher's Note